SiC-Based
High-Density Composite Electric Drivetrain Converters

Dragan Maksimovic

Colorado Power Electronics Center
ECEE Department, University of Colorado – Boulder
maksimov@colorado.edu

IEEE PELS San Francisco Bay Area Chapter Seminar, May 26, 2022

Outline

- **Application: Drivetrain Power Electronics Architectures**
- **Composite Converter Architectures**
- **Optimization of a 1200 V, 125 kW SiC Composite Converter**
  - Architecture
  - Partial-power modules: power-stage and planar magnetics
  - Controls for online module and system-level optimization
  - Thermal management and packaging
- **1200 V, 125 kW Prototype**
  - 21.3 kW/L density
  - 99% drive-cycle weighted efficiency

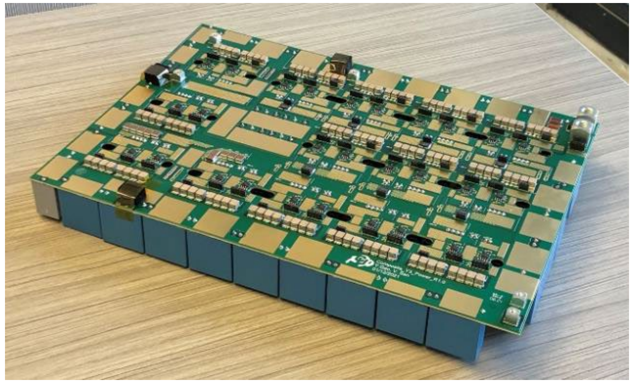

Power Electronics: Enabling Technology for Energy Efficiency and Renewable Energy

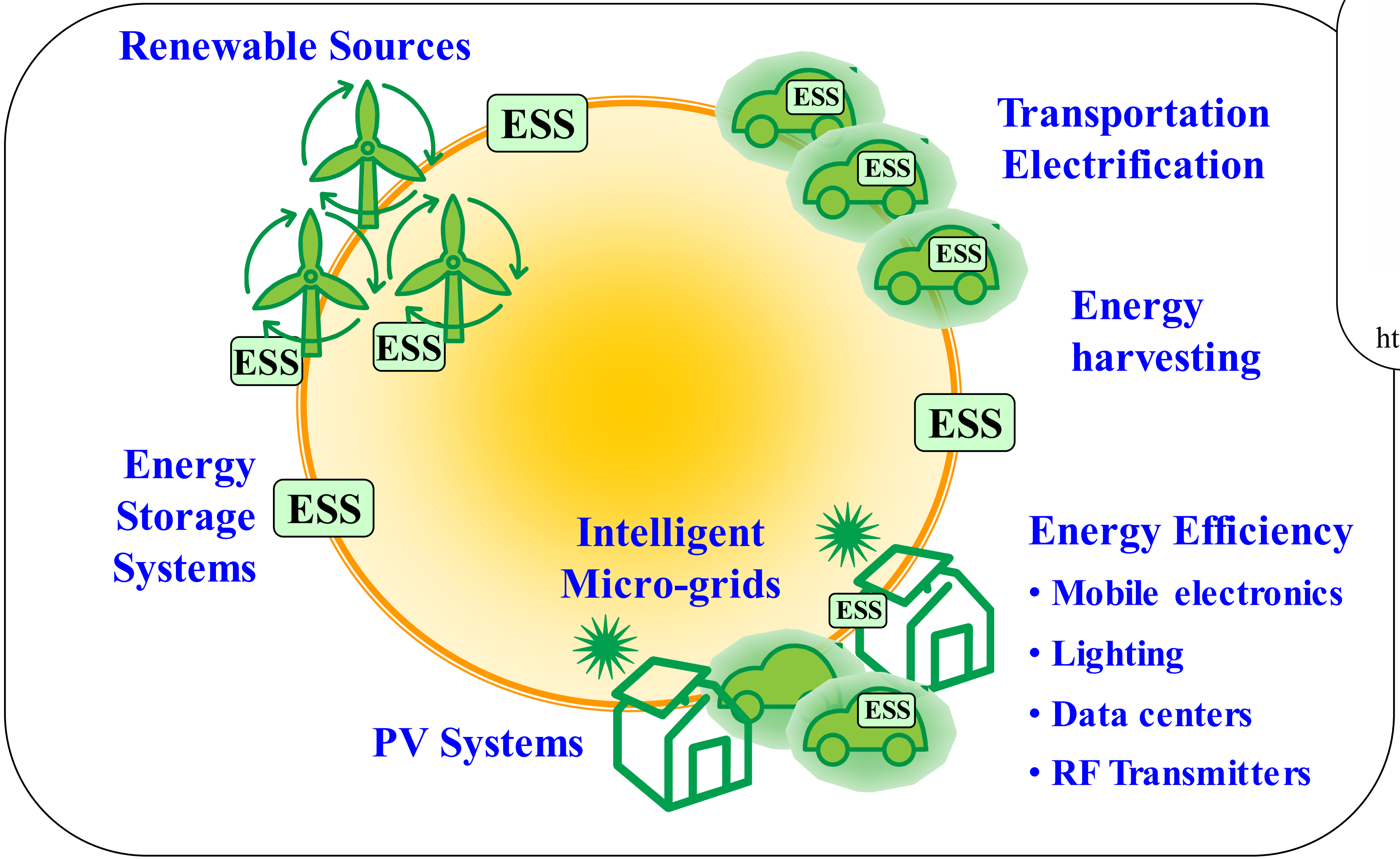

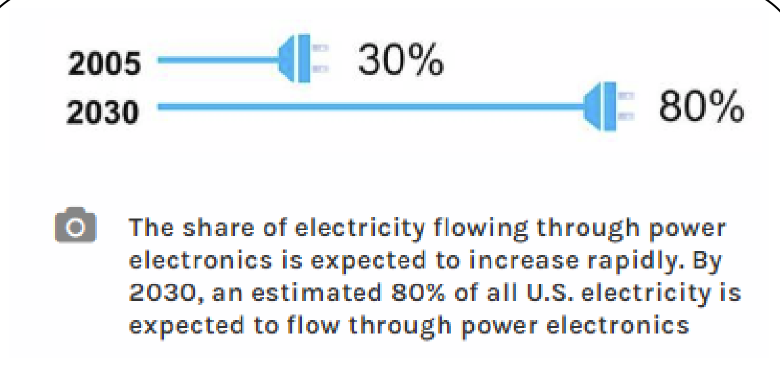

DOE Power America, https://www.energy.gov/eere/amo/power-america

Substantial impact on the society and the environment

Colorado Power Electronics Center (CoPEC)

- **Luca Corradini, Bob Erickson, Bri-Mathias Hodge, Dragan Maksimovic**
- **Research projects sponsored by industry and agencies** (DOE SETO, DOE VTO, ARPA-E, NSF, ONR, DARPA, …)
- **Power electronics education**
  - Fundamentals of Power Electronics 3rd edition
  - Undergraduate, MS and PhD programs
  - Comprehensive power electronics curriculum
  - Certificates in power electronics and electric drivetrain technology
  - Online MS-EE degree and short courses on Coursera

    https://www.colorado.edu/ecee/msee/curriculum/power-electronics

    Power Electronics Specialization: 4 short courses

    Modeling, Control of Power Electronics Specialization: 5 short courses

    Power Electronics Project Course

    Algorithms for Battery Management Systems Specialization: 5 short courses

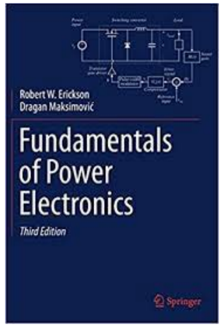

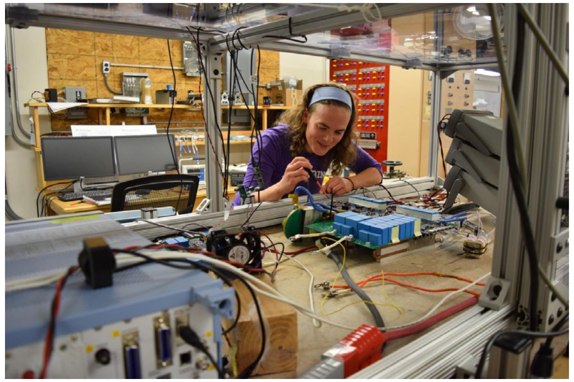

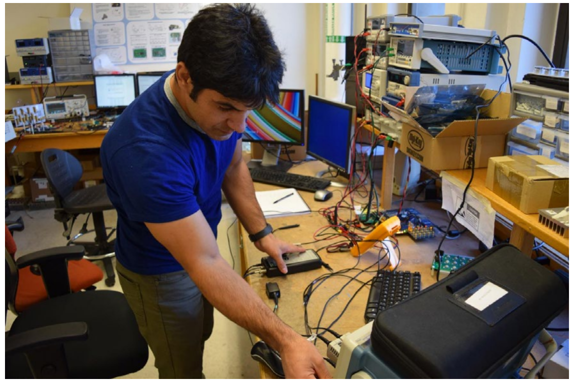

NSF Engineering Research Center

Advancing Sustainability through Powered Infrastructure for Roadway Electrification

Electric Vehicle and Roadway testbed at USU

UtahStateUniversity University of Colorado Boulder UTEP PURDUE UNIVERSITY

Convergent ASPIRE research thrusts

Power

Transportation

Adoption

Data

- More than 50 affiliated institutions and innovation partners including industry, national labs, DOTs, …
- Multiple large-scale demonstration projects including extreme fast charging and dynamic wireless charging

Outline

- **Application: Drivetrain Power Electronics Architectures**
- **Composite Converter Architectures**
- **Optimization of a 1200 V, 125 kW SiC Composite Converter**
  - Architecture
  - Partial-power modules: power-stage and planar magnetics
  - Controls for online module and system-level optimization
  - Thermal management and packaging
- **1200 V, 125 kW Prototype**
  - 21.3 kW/L density
  - 99% drive-cycle weighted efficiency

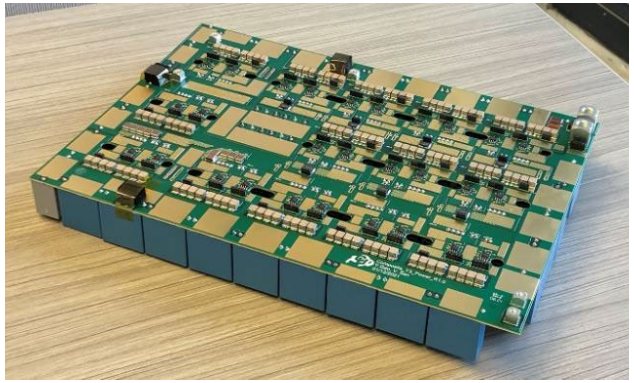

Application: Drivetrain Power Electronics Architecture

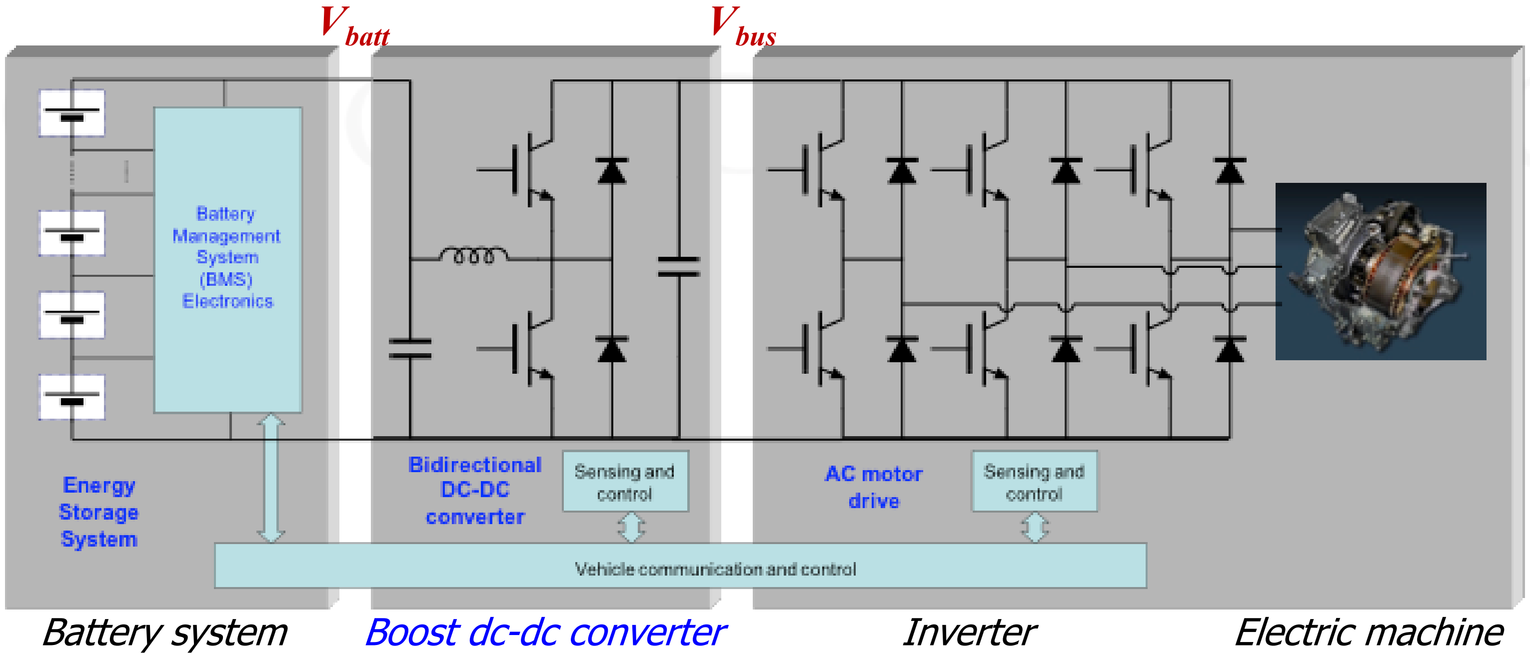

- xEV battery voltage V_{batt} (200-400 V), bus voltage V_{bus} (200-800 V)
- In some cases, a Boost dc-dc converter is inserted between the battery and the drive
    - Decouples battery system from the electric drive (inverter + machine) system
    - Offers system-level efficiency, size and safety advantages
    - Enables dynamic online V_{bus} adjustments in response to operating point

xEV Drivetrain Power Electronics: Conventional Realization

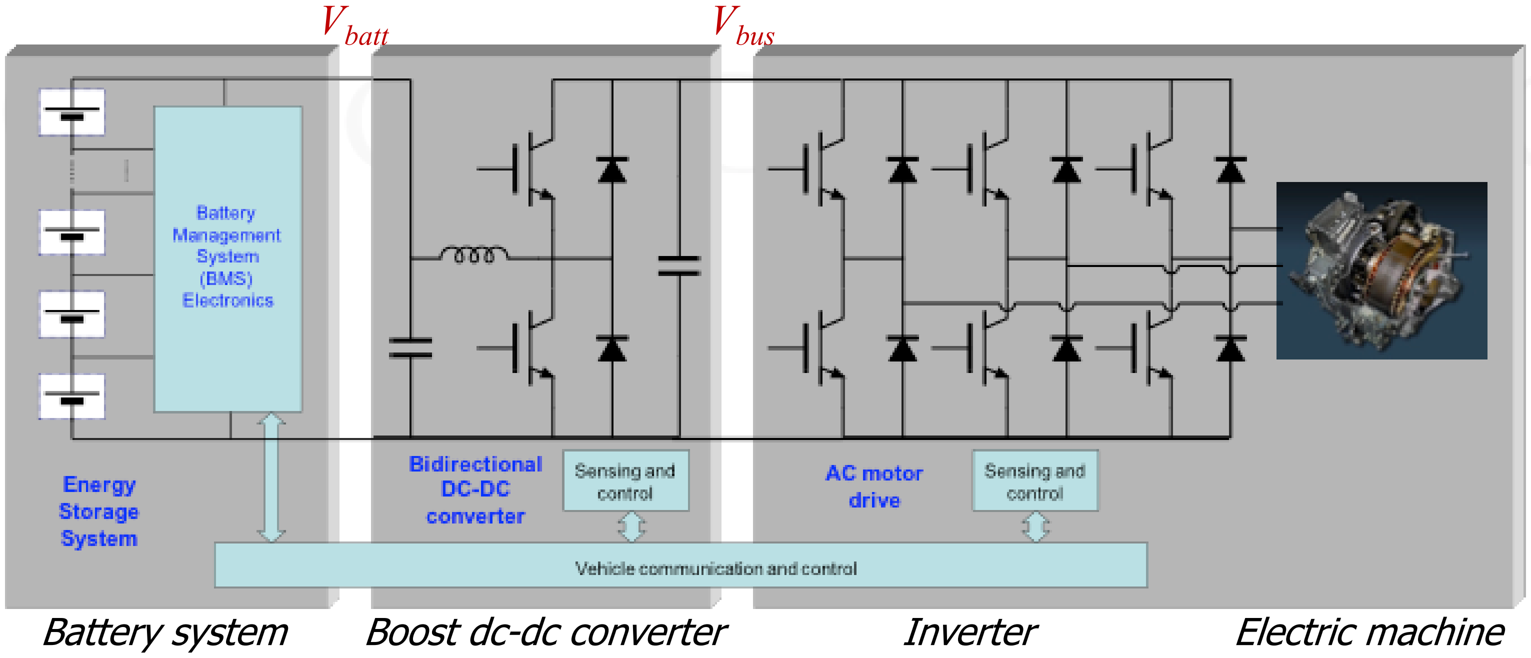

- IGBT-based power stage switching at 10's of kHz
- Boost CAFE*-weighted efficiency: 94.7%
- Boost power density: ~ 4 kW/L, primarily due to large *L* and *C* components

*Corporate average fuel economy (CAFE): a weighted drive cycle defines a typical system operating pattern

xEV Drivetrain Application: Distribution of Operating Points

US06 drive cycle example

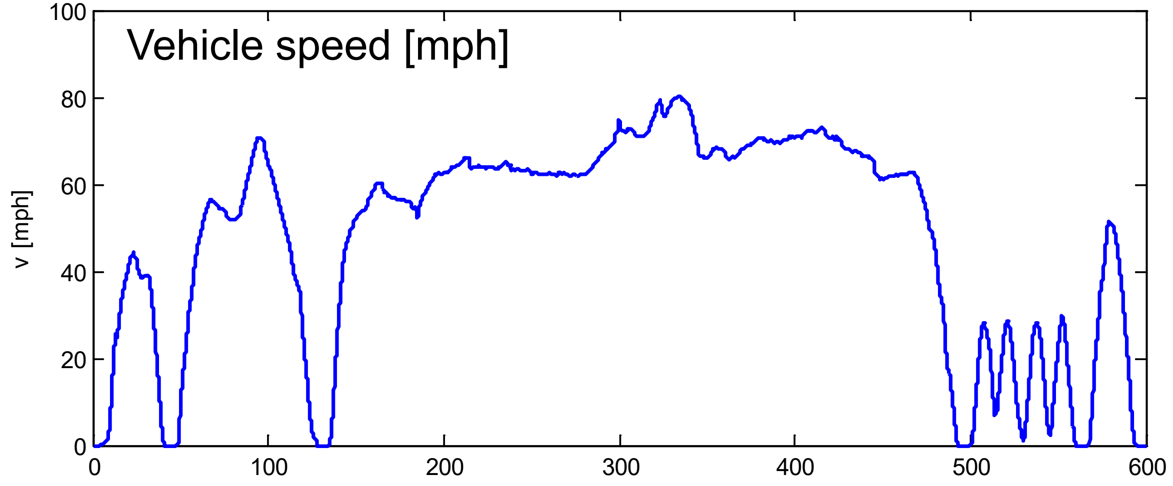

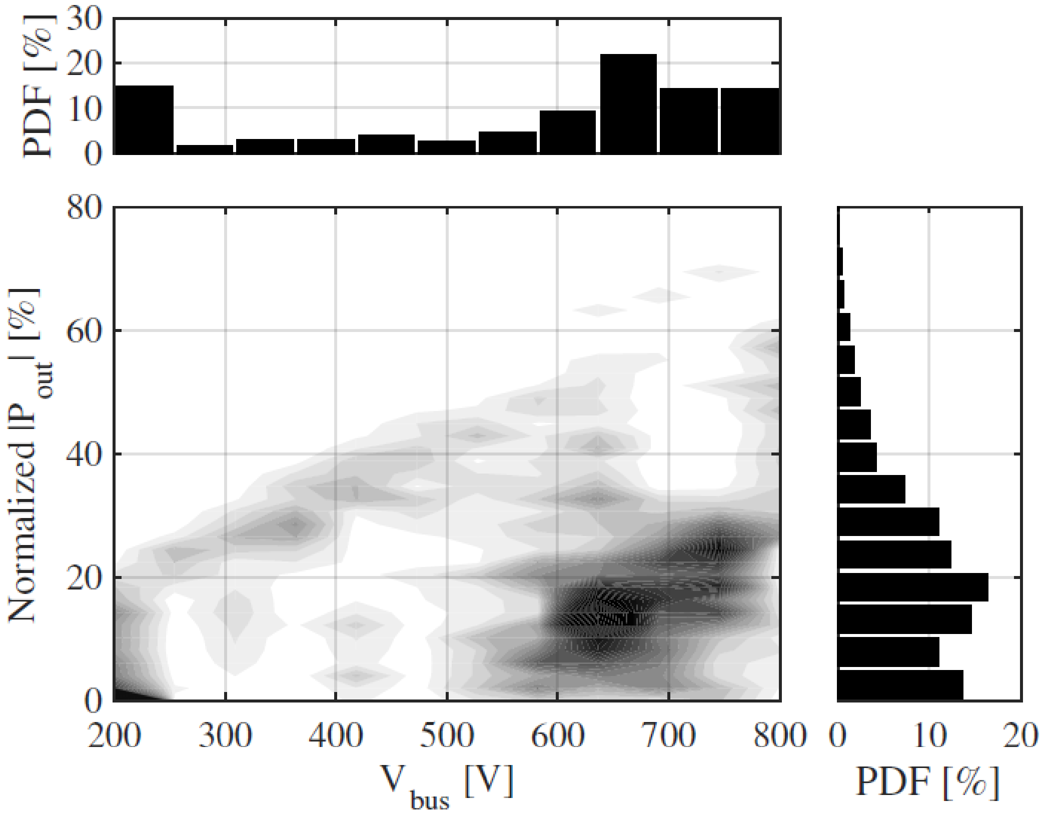

- Most of the time spent at relatively low power and at relatively high V_{bus}/V_{batt} step-up ratios
- Efficiency of the Boost converter is fundamentally limited at these operating points

$Q = P_{out} / P_{loss}$ is a Fundamental Measure of the Converter Quality

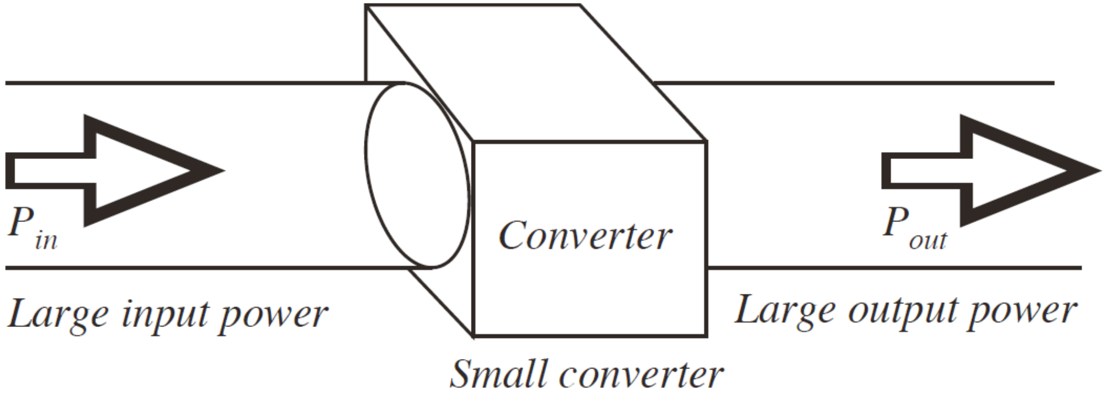

Large Q implies that the converter elements can be packaged with high density and a small cooling system, leading to a converter of small size and weight, and of low temperature rise

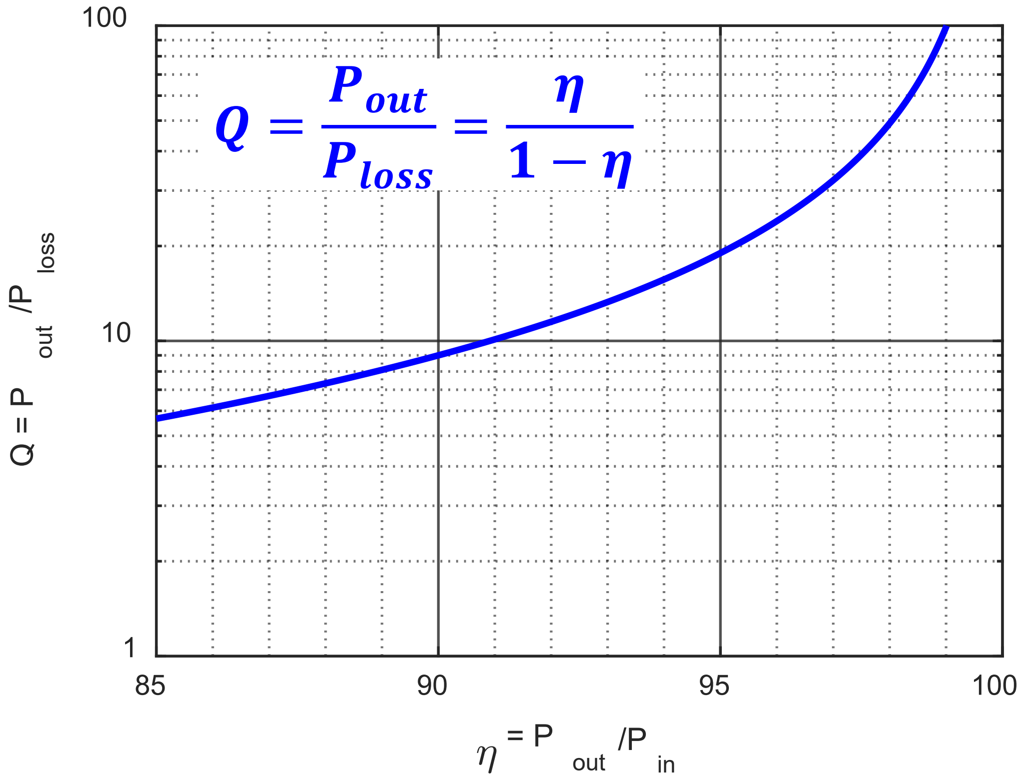

xEV Drivetrain Power Electronics: Conventional Realization

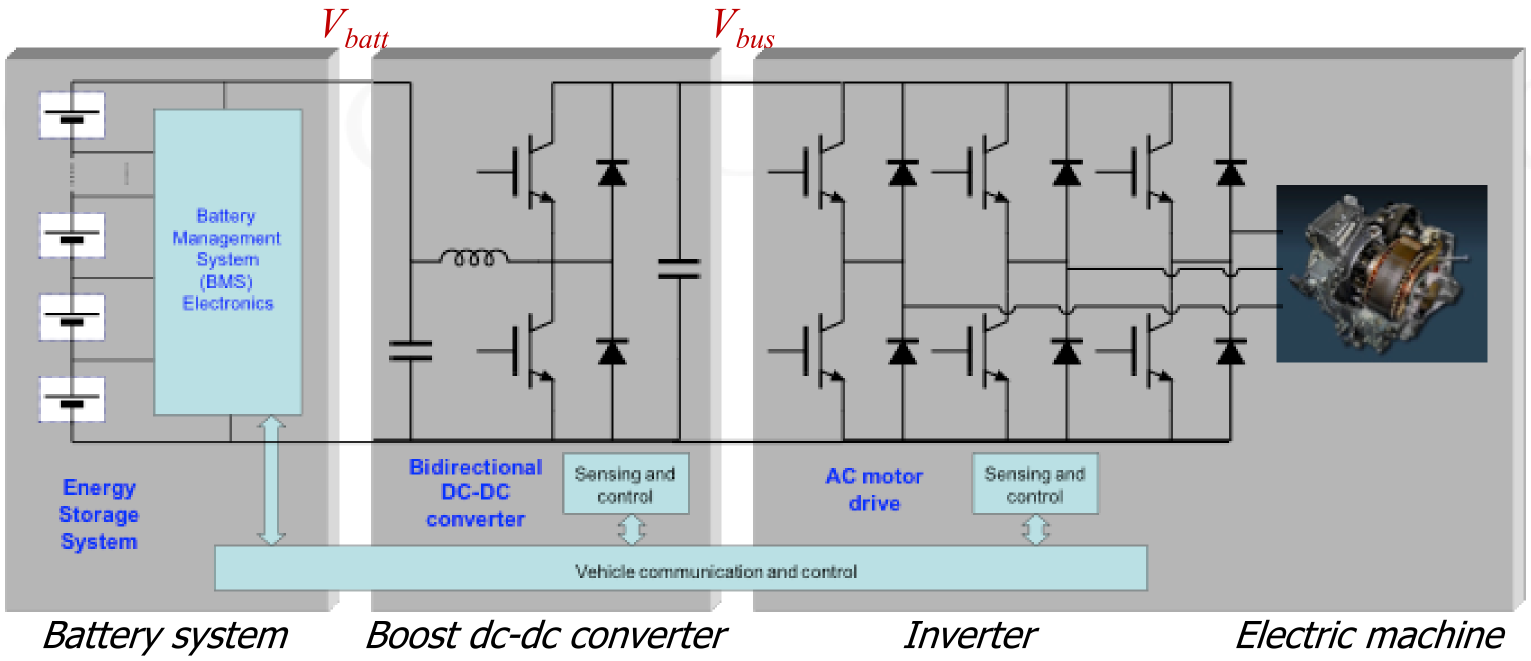

- IGBT-based power stage switching at 10's of kHz
- Boost CAFE*-weighted efficiency: 94.7%, **converter quality factor: $Q = 18$**
- Boost power density: ~ 4 kW/L, primarily due to large L and C components

*Corporate average fuel economy (CAFE): a weighted drive cycle defines a typical system operating pattern

Drivetrain Power Electronics: Trends

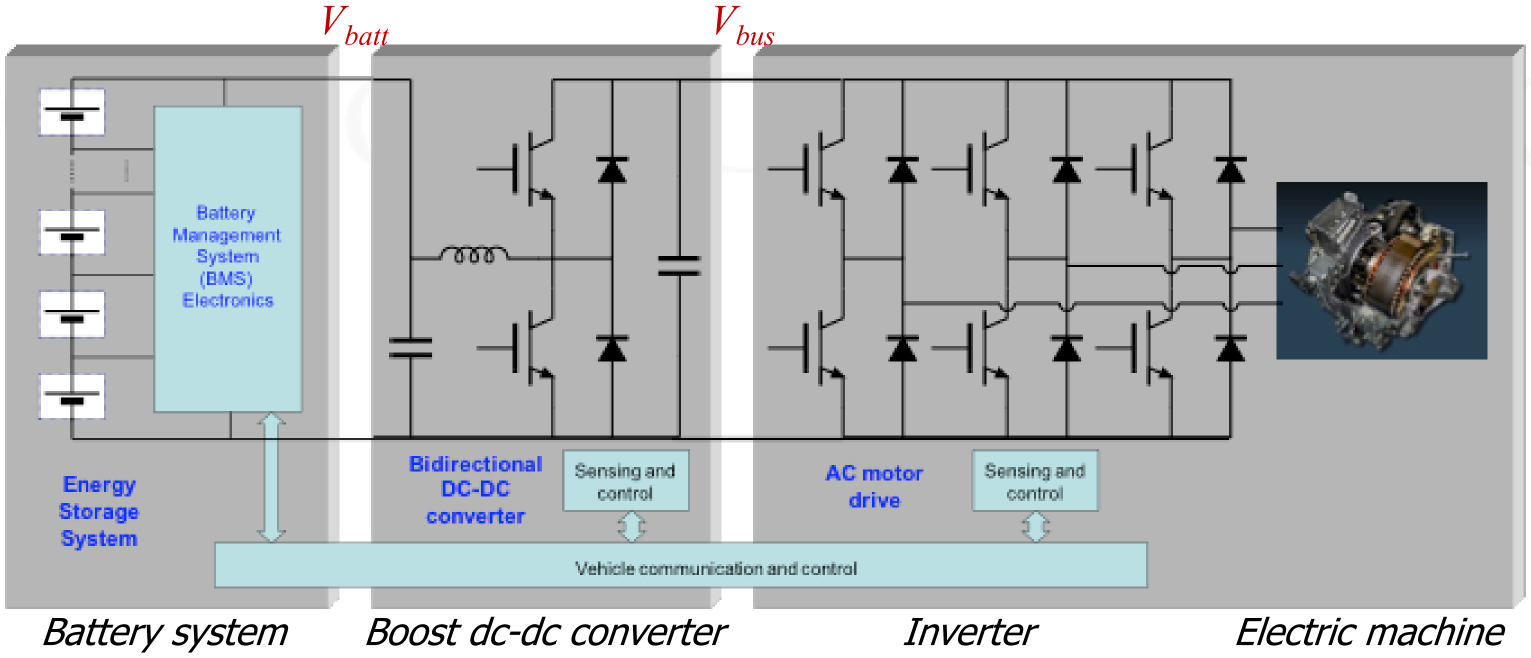

- Power density and drive-cycle weighted quality factor Q improvements
- Operating voltages in xEV and electrified aircraft drivetrain systems are moving up
  - Battery systems moving to V_{batt} = 800 V
  - Bus voltage: xEV V_{bus} = 1200 V, electrified aircraft V_{bus} = medium voltage (kV's)

Trend (Conventional): Replace IGBT's with SiC MOSFETs

SiC-based 1200 V, 100 kW conventional Boost design example

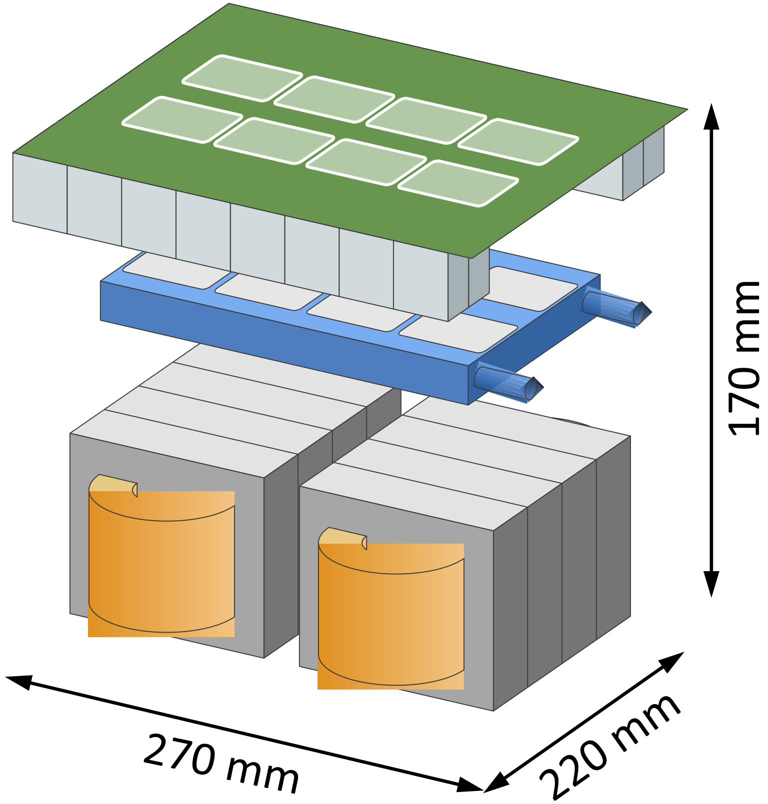

*Corporate average fuel economy (CAFE): a weighted drive cycle defines a typical system operating pattern

	SiC conventional boost	Improvements vs. IGBT boost
Max output voltage	**1200 V**	**50% higher**
Switching frequency	60 kHz	**3-6x higher**
Magnetics	Wire-wound	**3x smaller**
Capacitors	Film	same
Power devices	1700 V SiC	
SiC semi area	1,600 mm^2	
CAFE Q	**63.5**	**3x higher**
CAFE Efficiency	**98.4%**	
Power density	**9.9 kW/L**	**2x higher**

Is There a Better Boost Architecture?

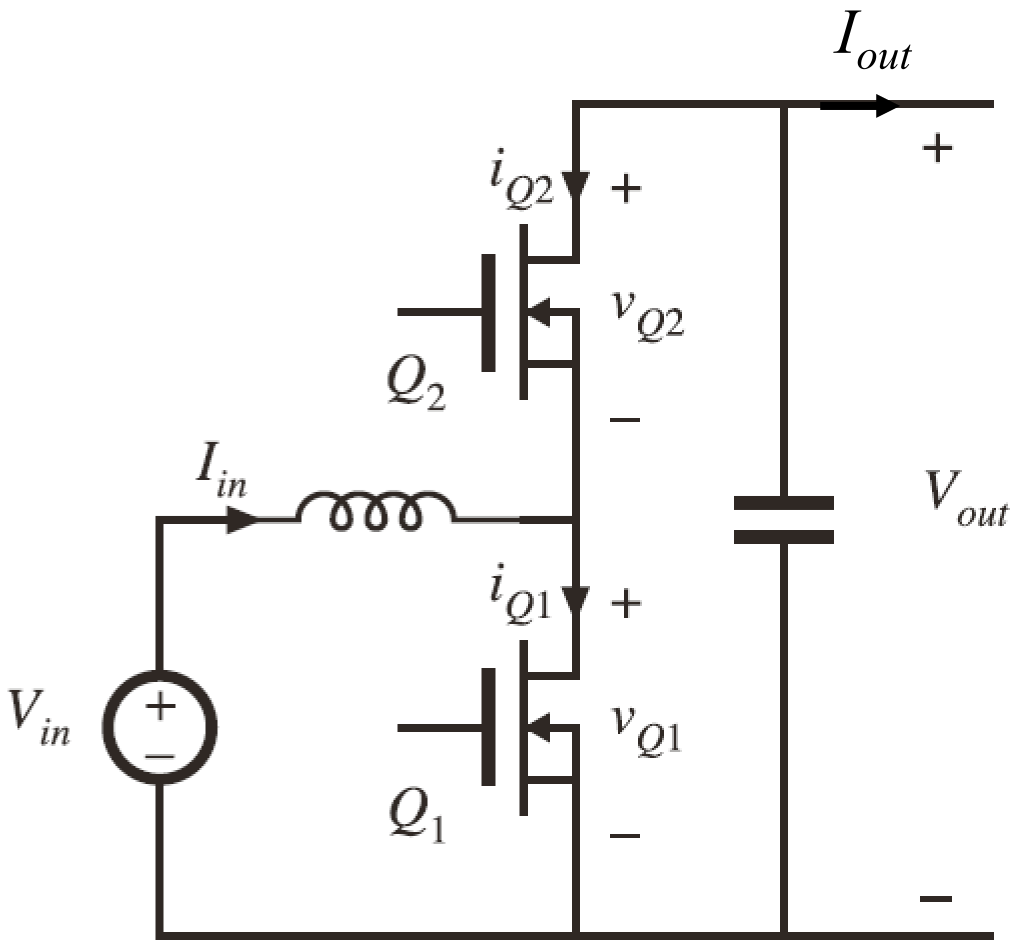

Is There a Better Boost Architecture?

Averaged-switch boost converter model

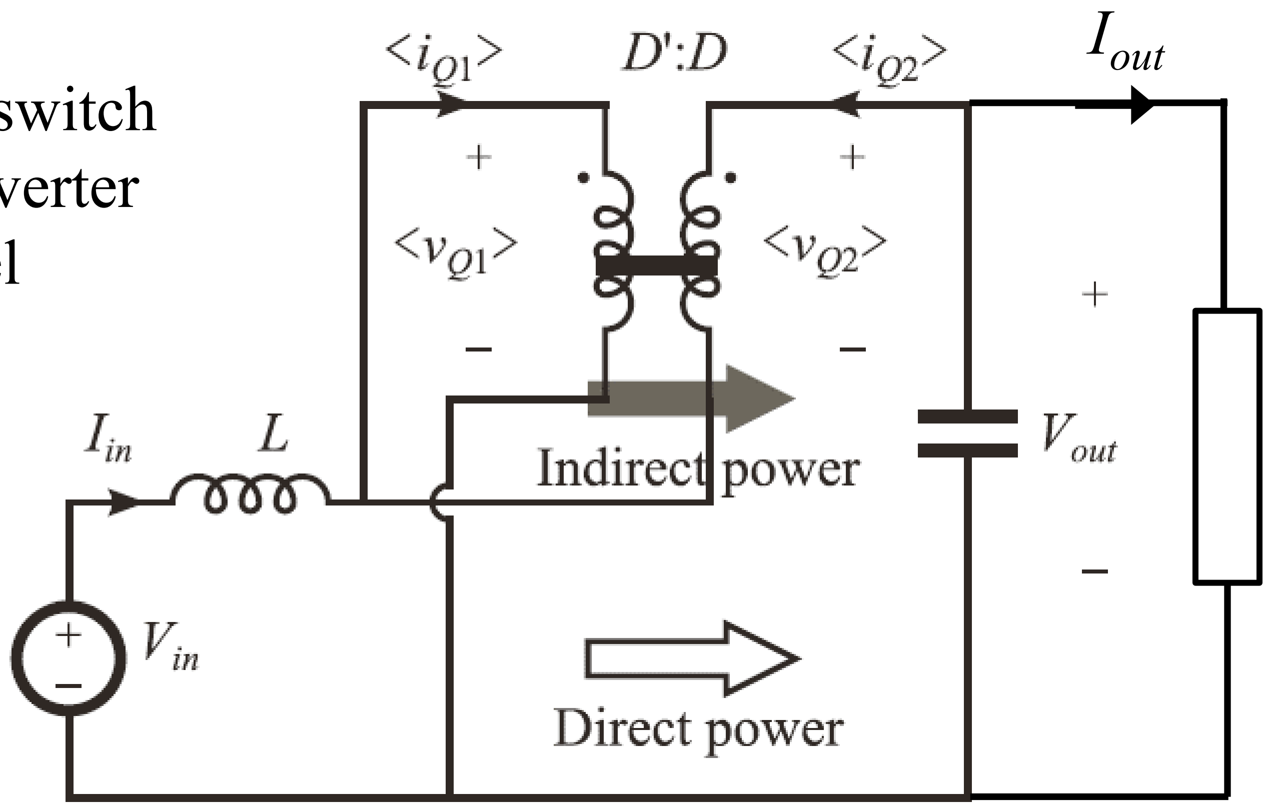

- Indirect power is the amount of power processed by the switches, dc-to-ac by the inverter switch Q_1, and ac-to-dc by the rectifier switch Q_2
- Fundamental mechanism by which Boost converter develops voltage gain
- Indirect power processing incurs both dc and ac (switching and magnetics) losses

Construction of a “Better” Boost Converter

Replace with a more efficient indirect power processor

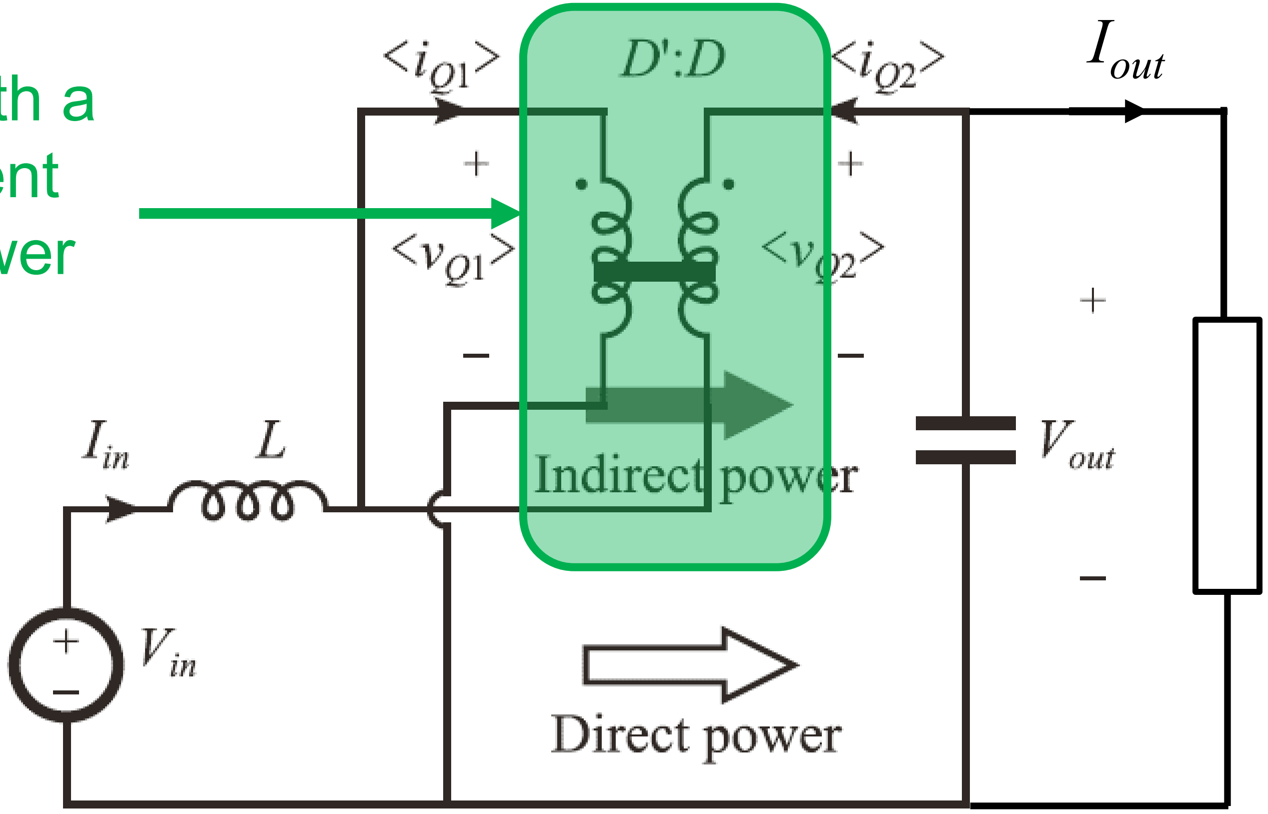

Composite Approach to Converter Architectures

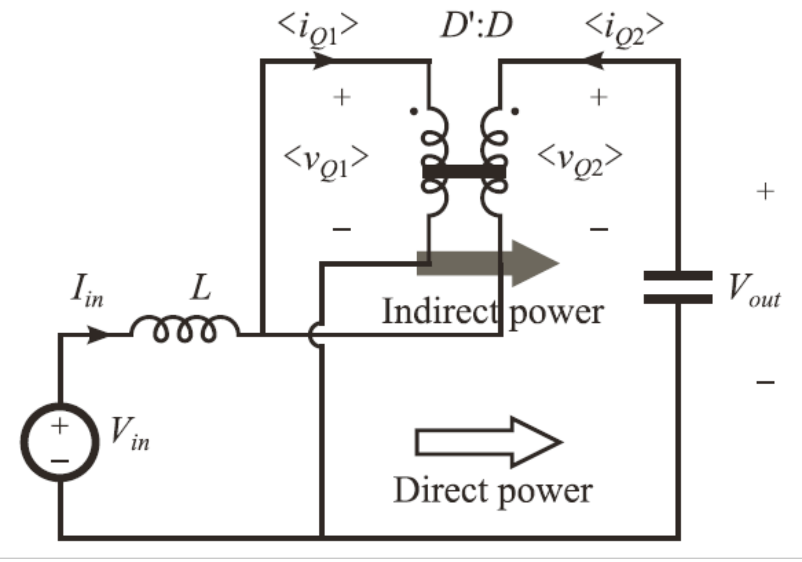

DC averaged model of the standard boost converter

Partial-power DCX module: efficient indirect power processor

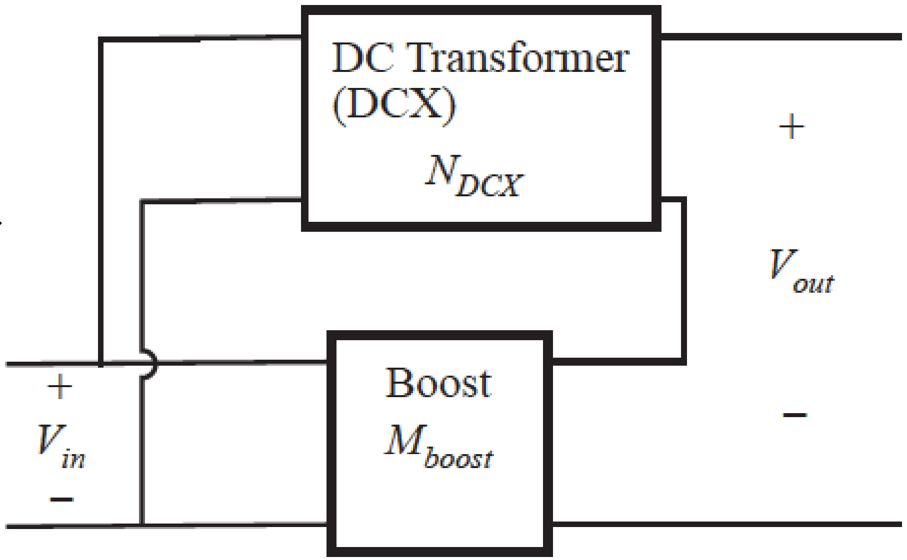

Partial-power boost module operates with much reduced step-up ratio

$$M = M_{boost} + N_{DCX}$$

Composite Approach to Converter Architectures

Composite converters: arrangements of ***dissimilar*** partial-power modules

DAB or LLC based high-efficiency,
≈ fixed conversion ratio converter, “DCX”

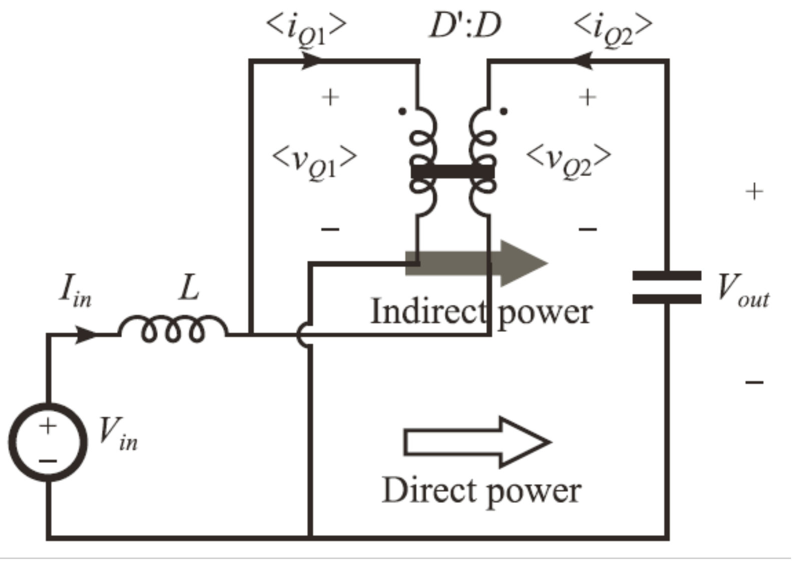

DC averaged model
of the standard boost
converter

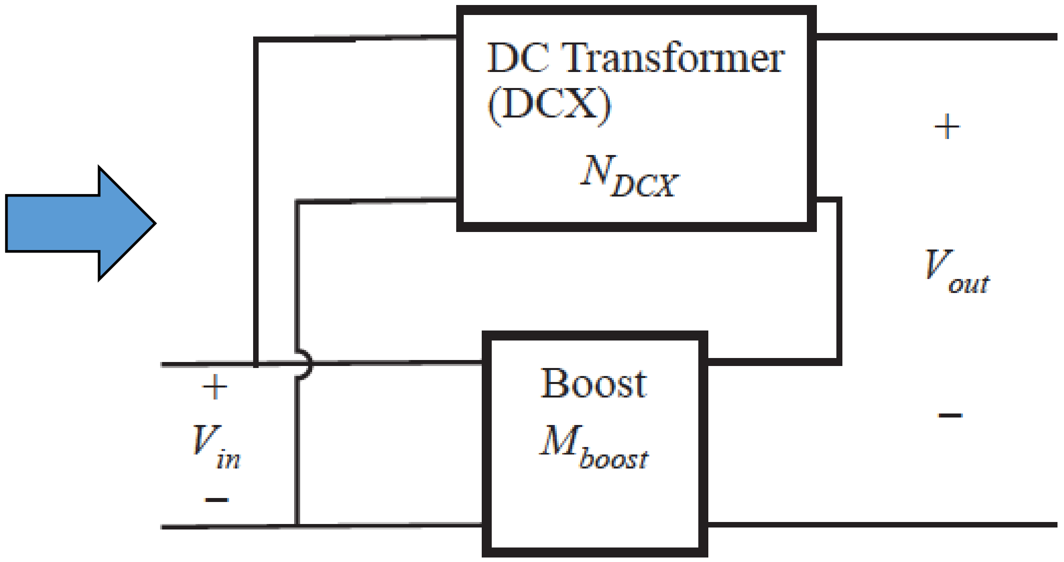

$$M = M_{boost} + N_{DCX}$$

Composite Converter: Illustration of the Basic Idea

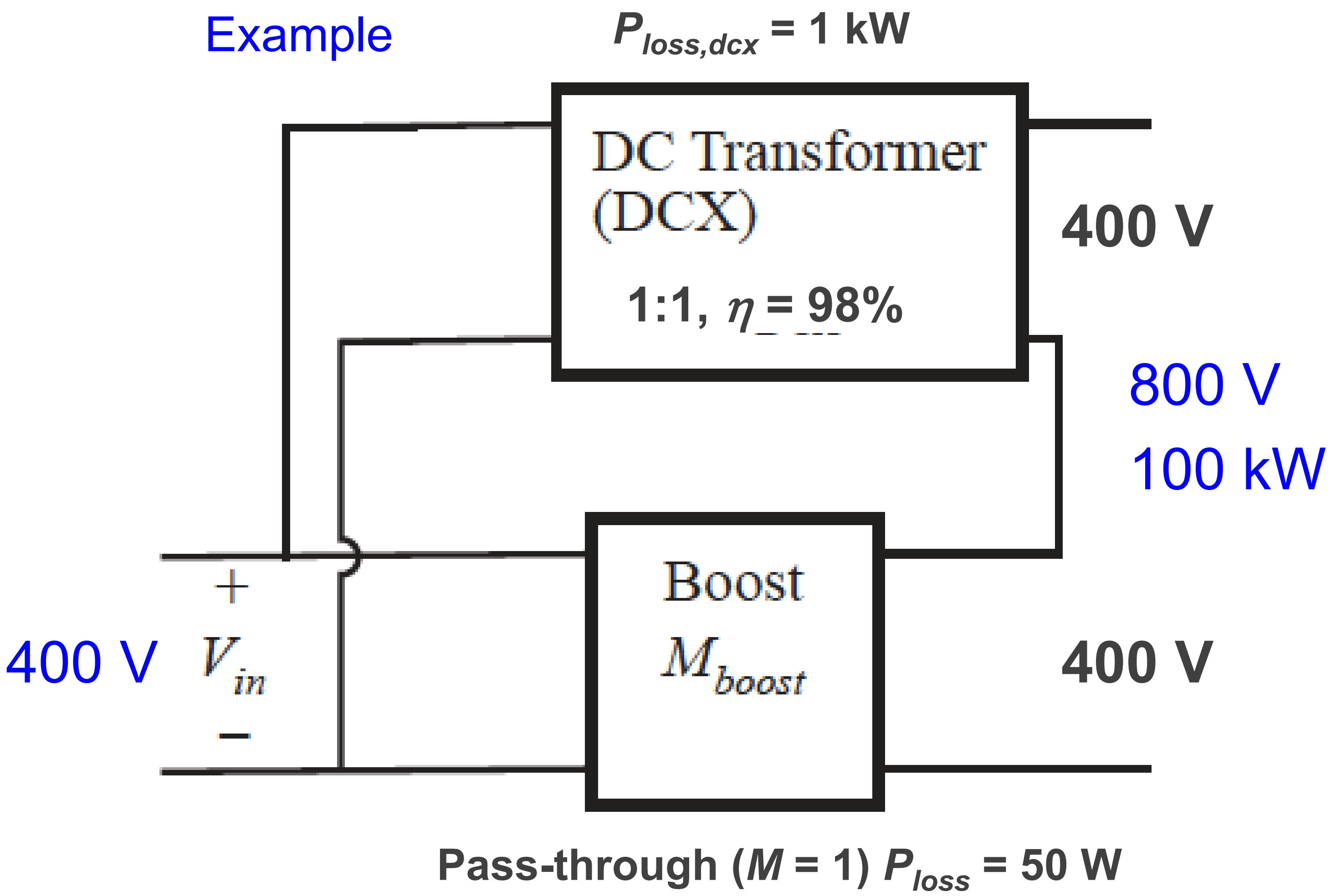

System efficiency: 99%

System Q = 95.2

Composite Converter: Illustration of the Basic Idea

- Component stresses are reduced
- Soft switching enables high efficiency at increased switching frequency
- Size of magnetics is reduced
- Capacitor RMS currents are reduced
- Major loss mechanisms are addressed

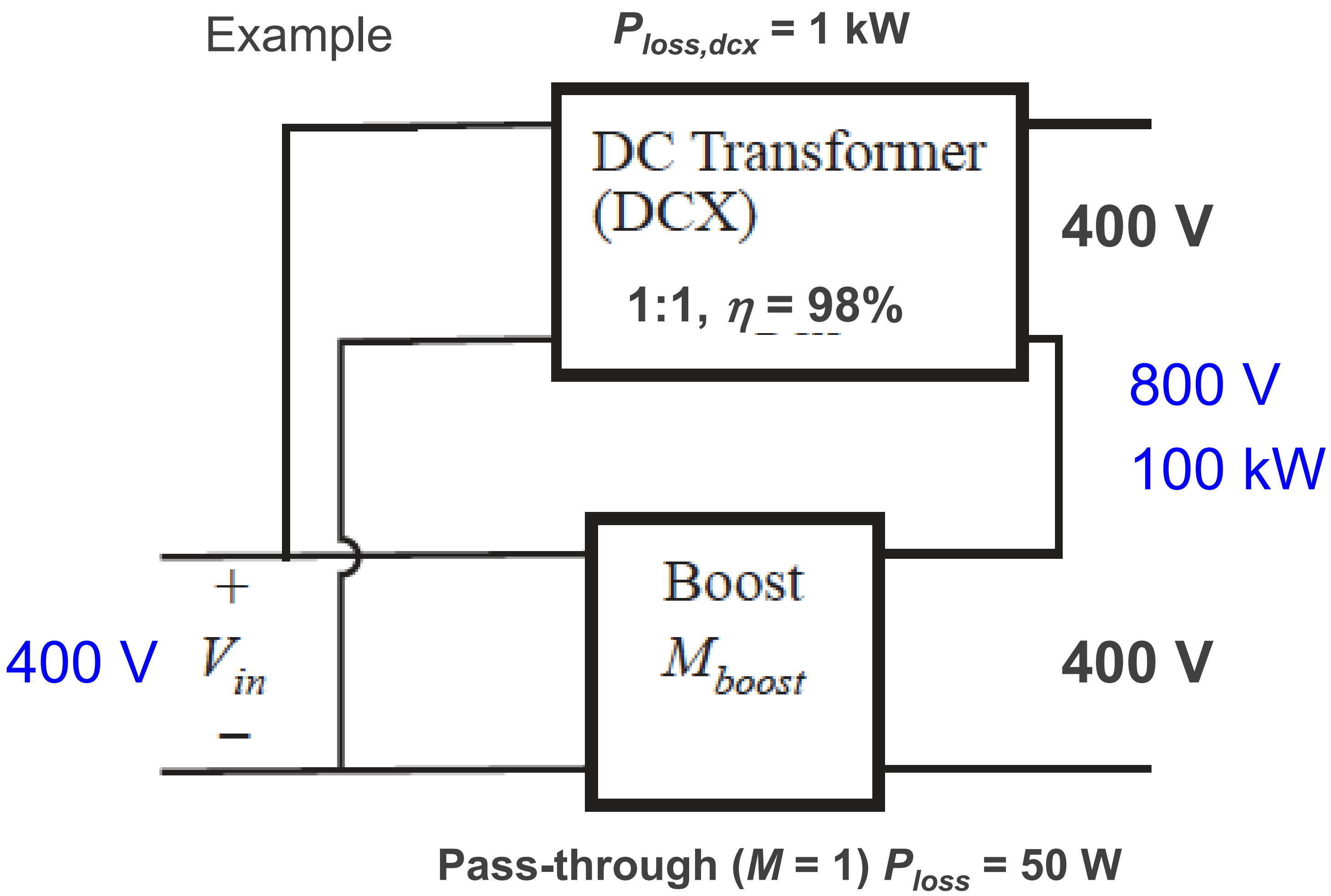

System efficiency: 99%

System Q = 95.2

Optimization of a 1200 V, 125 kW SiC Composite Converter

- Architecture
- Partial-power converter modules: power-stage and planar magnetics
- Controls for online module and system-level optimization
- Thermal management and packaging

Optimization of a 1200 V, 125 kW SiC Composite Converter

- Architecture
- Partial-power converter modules: power-stage and planar magnetics
- Controls for online module and system-level optimization
- Thermal management and packaging

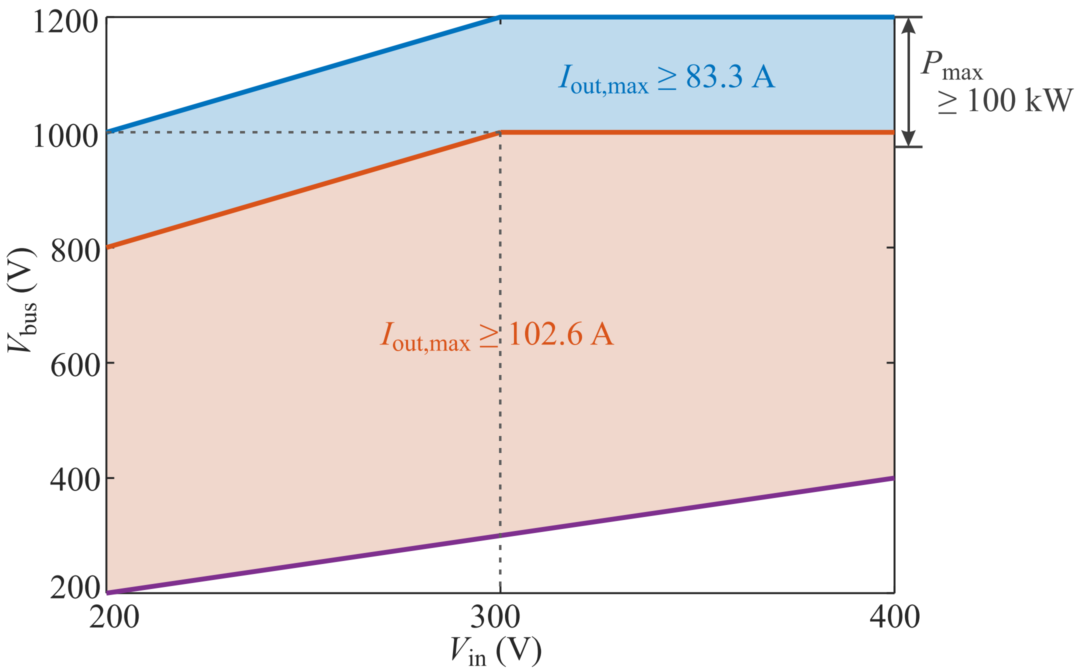

Operating specifications

- $P_{max} \geq 100$ kW
- $V_{mout,max} = 1200$ V
- $V_{in,nom} = 350$ V
- $T_{amb} = 65$ °C

SiC MOSFETs

- Wolfspeed 900 V SiC-MOSFETs (Gen 3)
- HT-4000 half-bridge package

Drive-cycle (CAFE) Operating Points

Time-domain drive-cycle velocity profiles

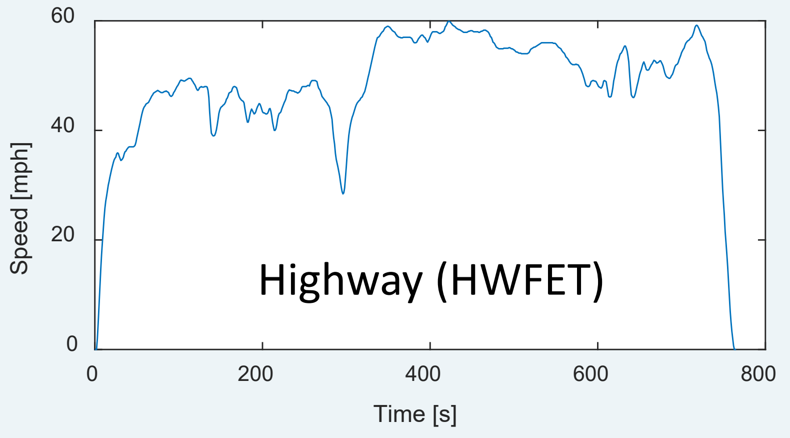

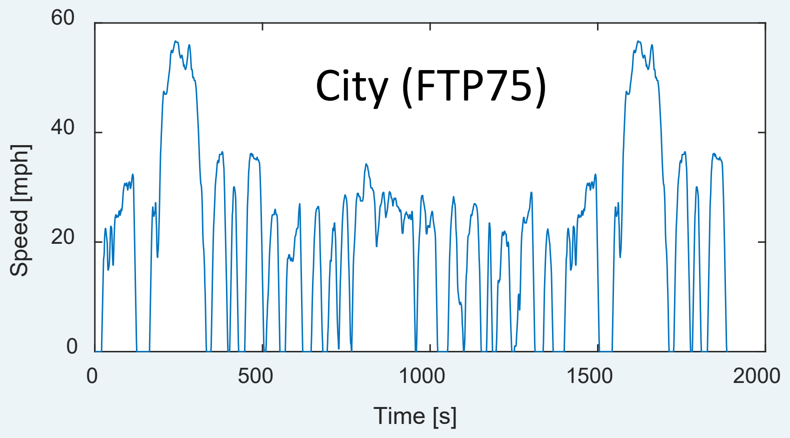

Comprehensive electro-mechanical Simulink model

Distribution of operating points

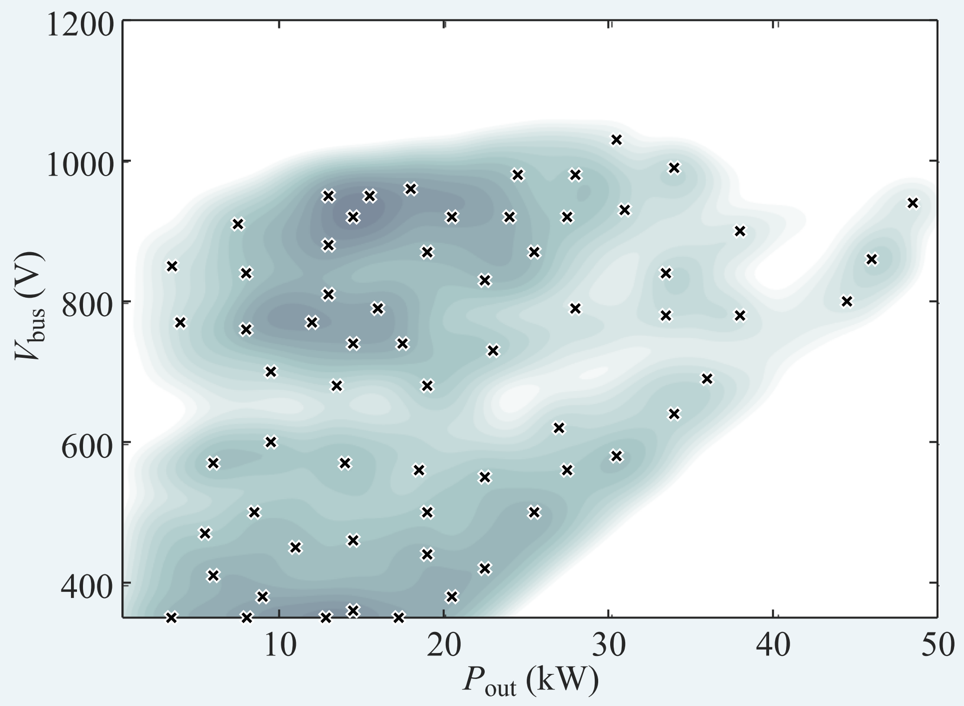

- Combined FTP-75 & HWFET
- 64 points considered in the design process
- More sampling points in high-probability areas

Y. Gao, V. Sankaranarayanan, E. M. Dede, A. Ghosh, D. Maksimovic and R. W. Erickson, "Drive-Cycle Optimized 99% Efficient SiC Boost Converter Using Planar Inductor with Enhanced Thermal Management," IEEE COMPEL 2019

Candidate Composite Architectures

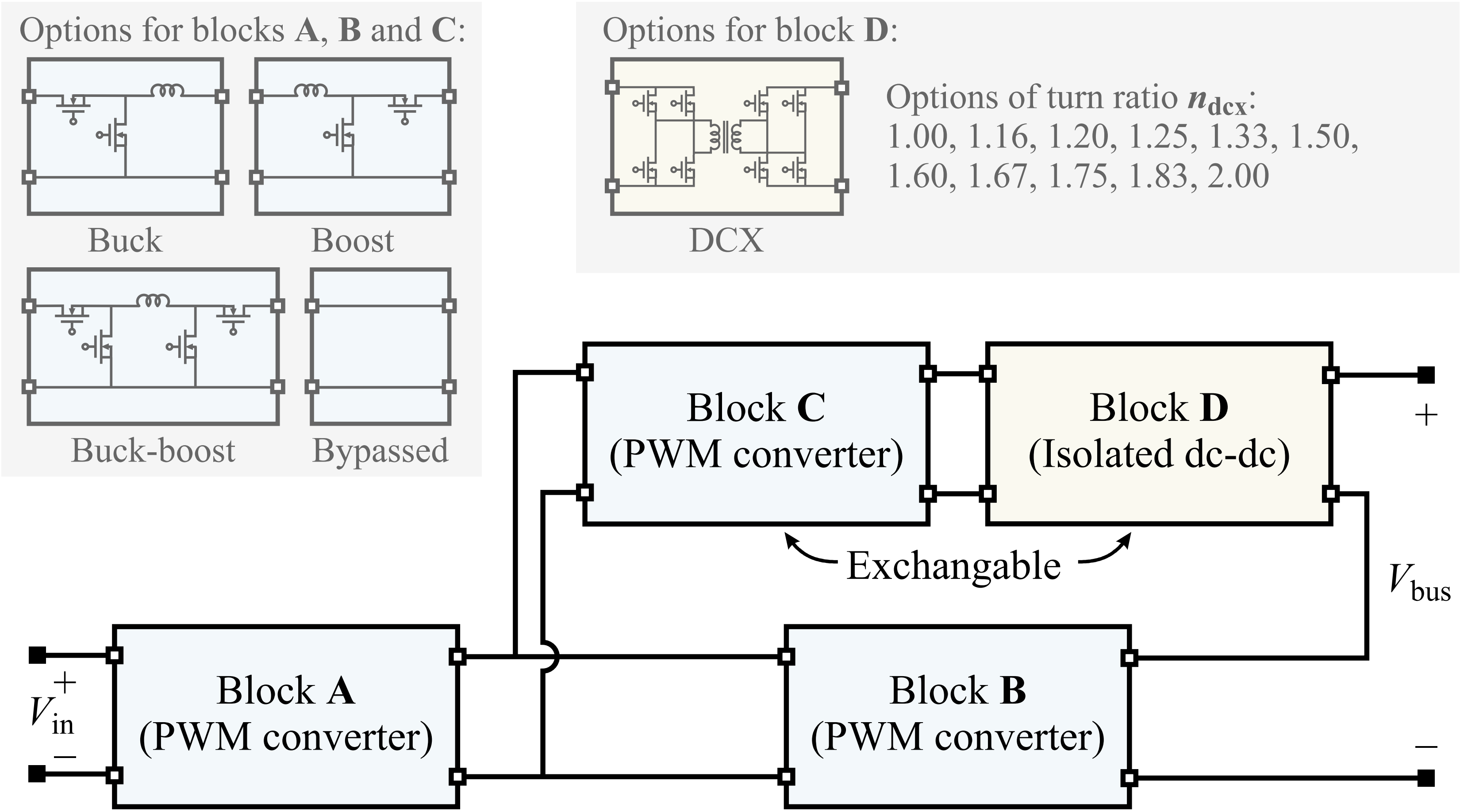

350 V

(200-400 V)

1200 V

125 kW

(200-1200 V)

Two-leg Composite Boost DC-DC Converter

Architecture Optimization: Design Space is Very Large

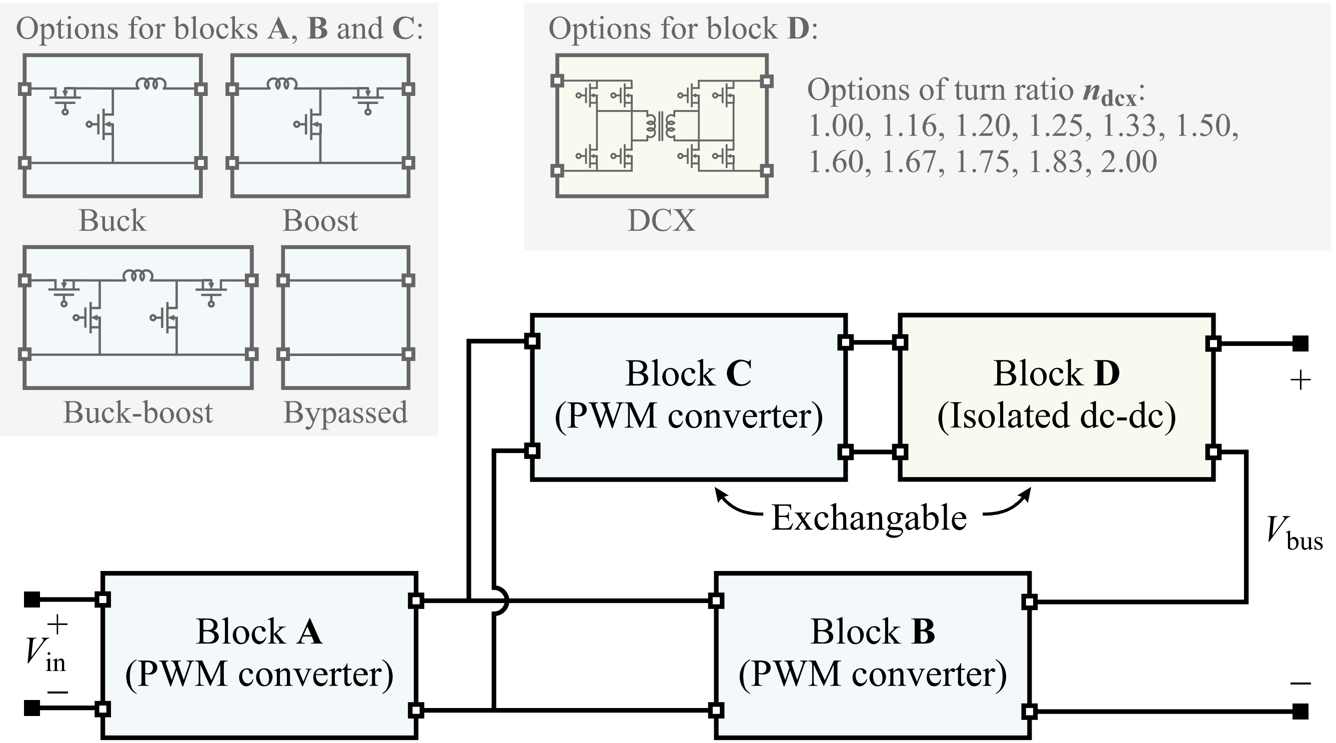

Two-leg composite architecture

- 4 × 4 × 4 × 11 × 2 = 1408 options
- 118 non-redundant options

Converter module design

- # of phases
- # of die per switch position
- Inductance
- Core size
- # of stacking cores
- # of turns
- Copper thickness

… (at least) 28 parameters per architecture

Optimization by exhaustive search over parameters

3 options for each variable: $118 \times 3^{28} = 2.7 \times 10^{15}$ designs to evaluate, not practical!

Hierarchical Data-driven Optimization Approach

Partial-power module designs and a module-level Pareto front

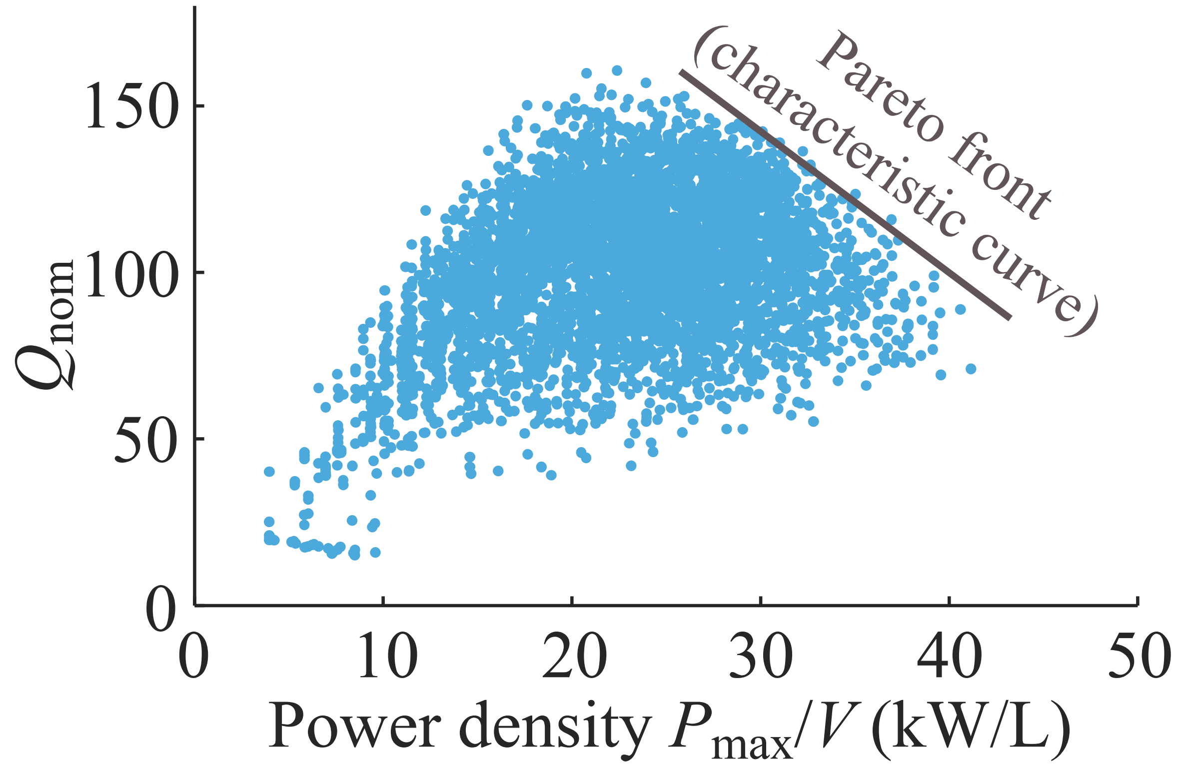

- Perform sweeps over design variables at the partial-power module level

Hierarchical Data-driven Optimization Approach

Partial-power module designs and a module-level Pareto front

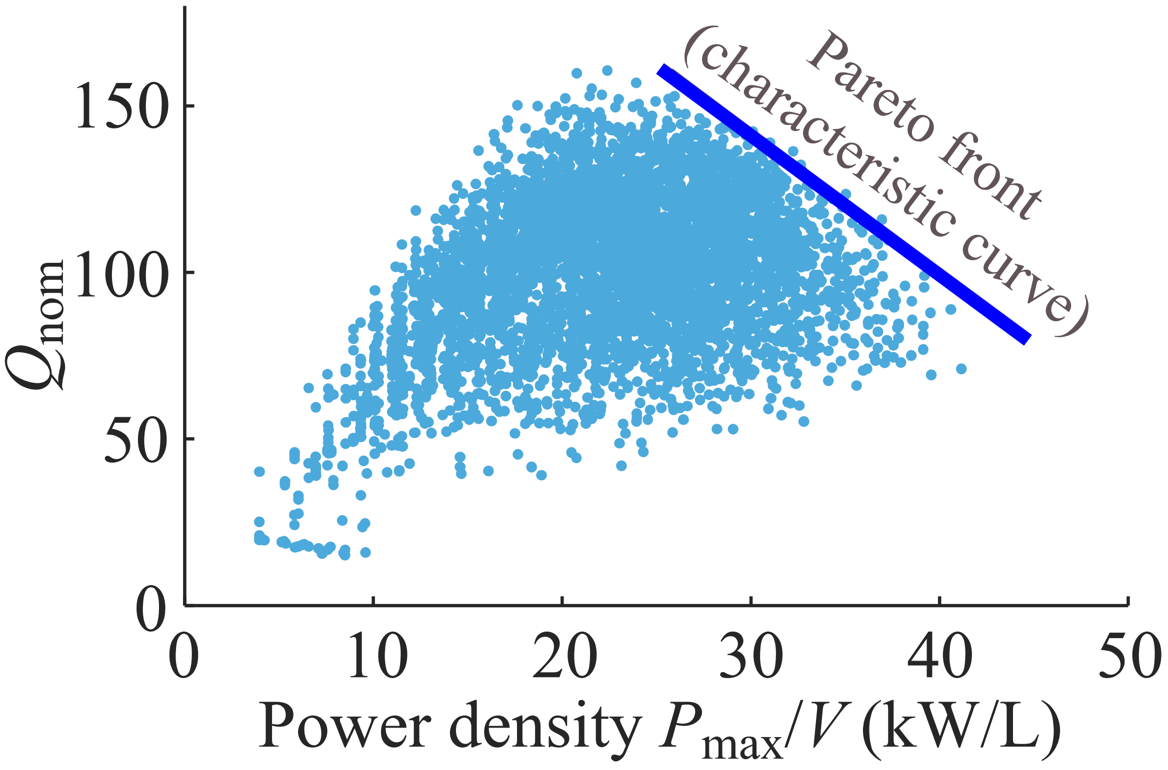

- Perform sweeps over design variables at the partial-power module level
- Capture the module-level Pareto front representing *Q* versus Power Density trade-off

Hierarchical Data-driven Optimization Approach

Partial-power module designs and a module-level Pareto front

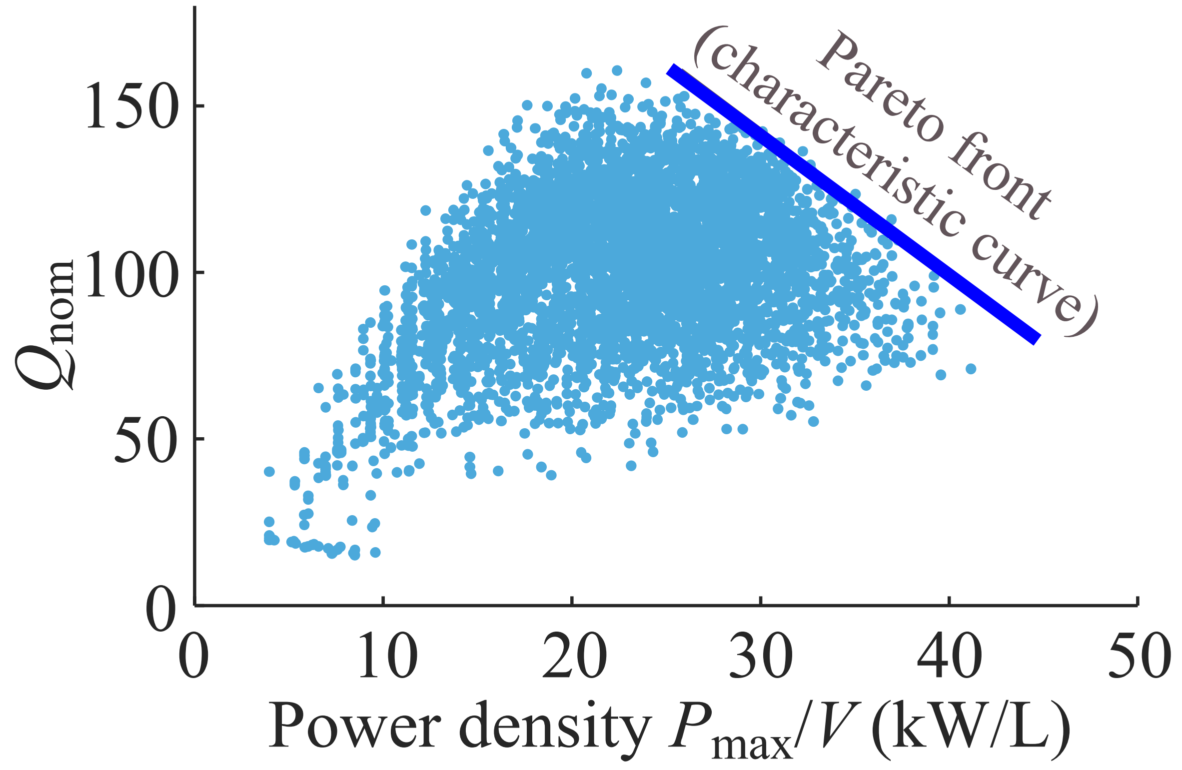

- Perform sweeps over design variables at the partial-power module level
- Capture the module-level Pareto front representing Q versus Power Density trade-off
- Combine module-level Pareto-fronts to identify the optimum composite architecture

Architecture-Level Optimization Goals: Q > 60, Power Density > 20 kW/L

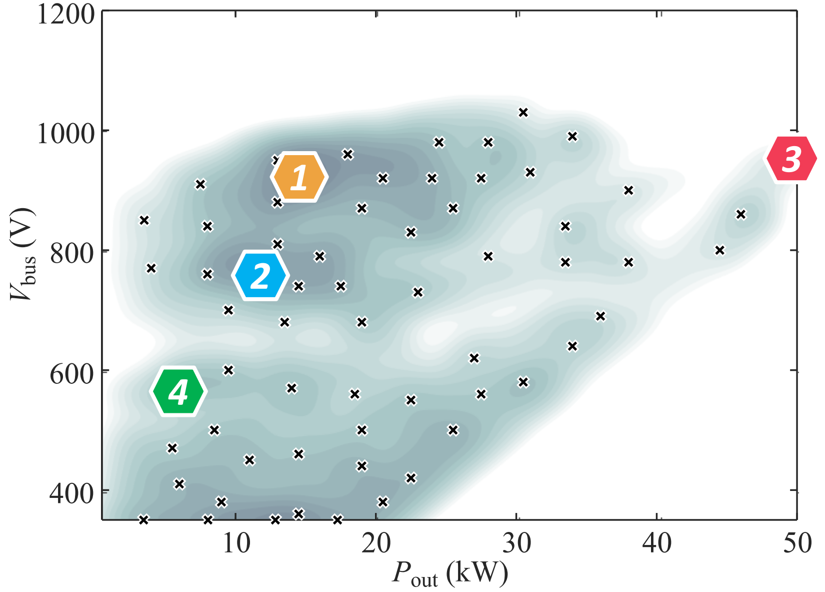

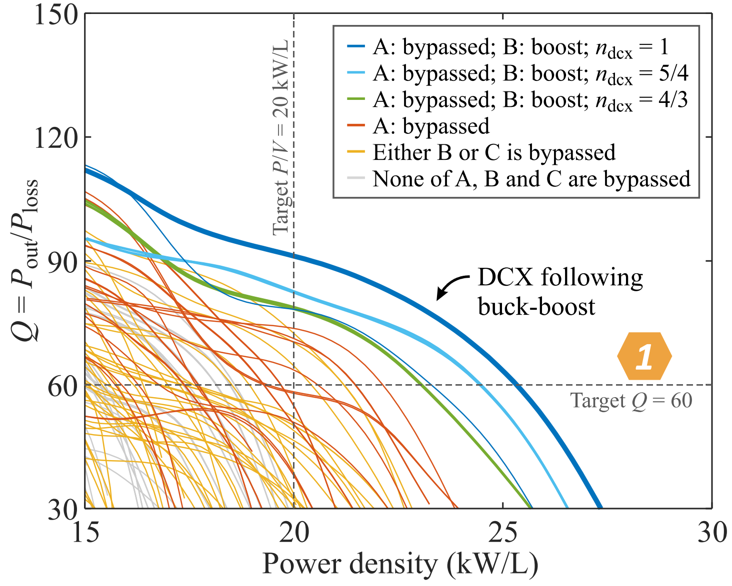

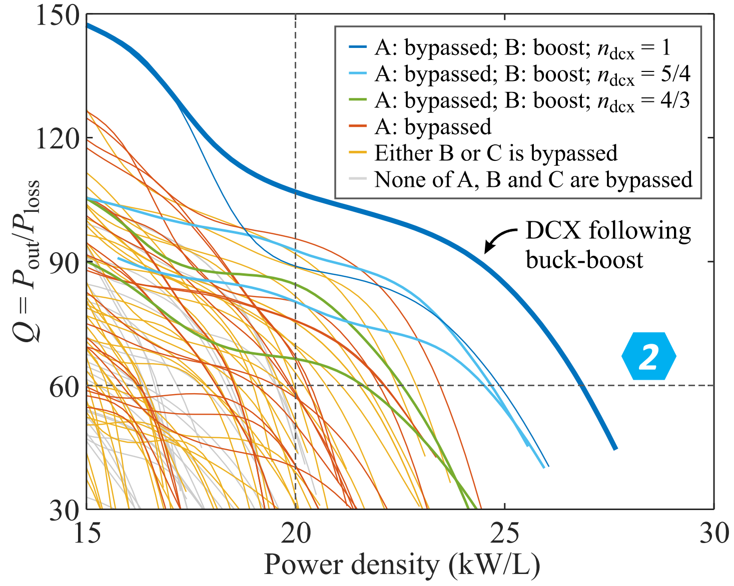

The optimal architecture

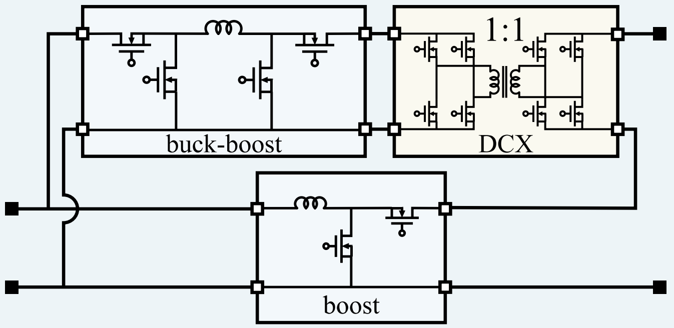

Optimal: n_{dcx} = **1**

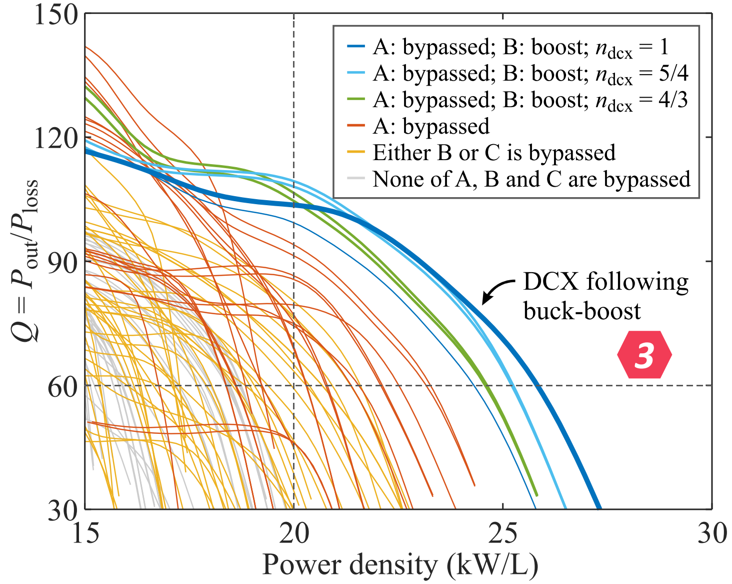

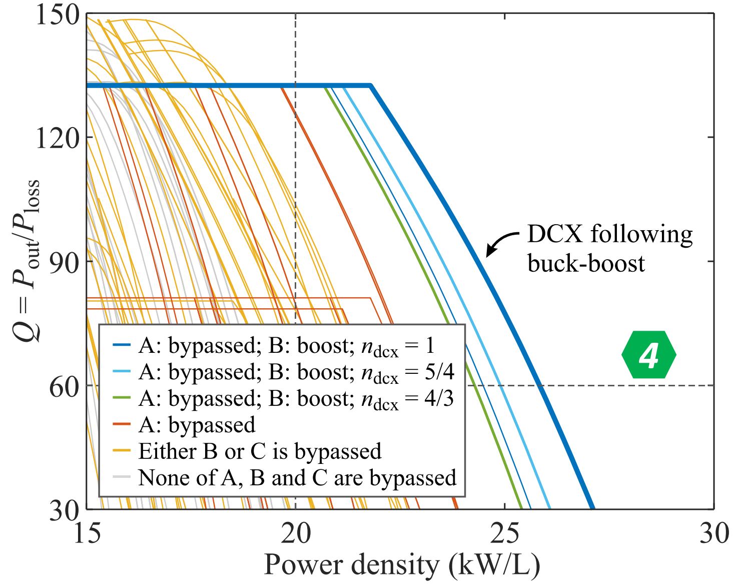

The Selected Composite Converter Architecture

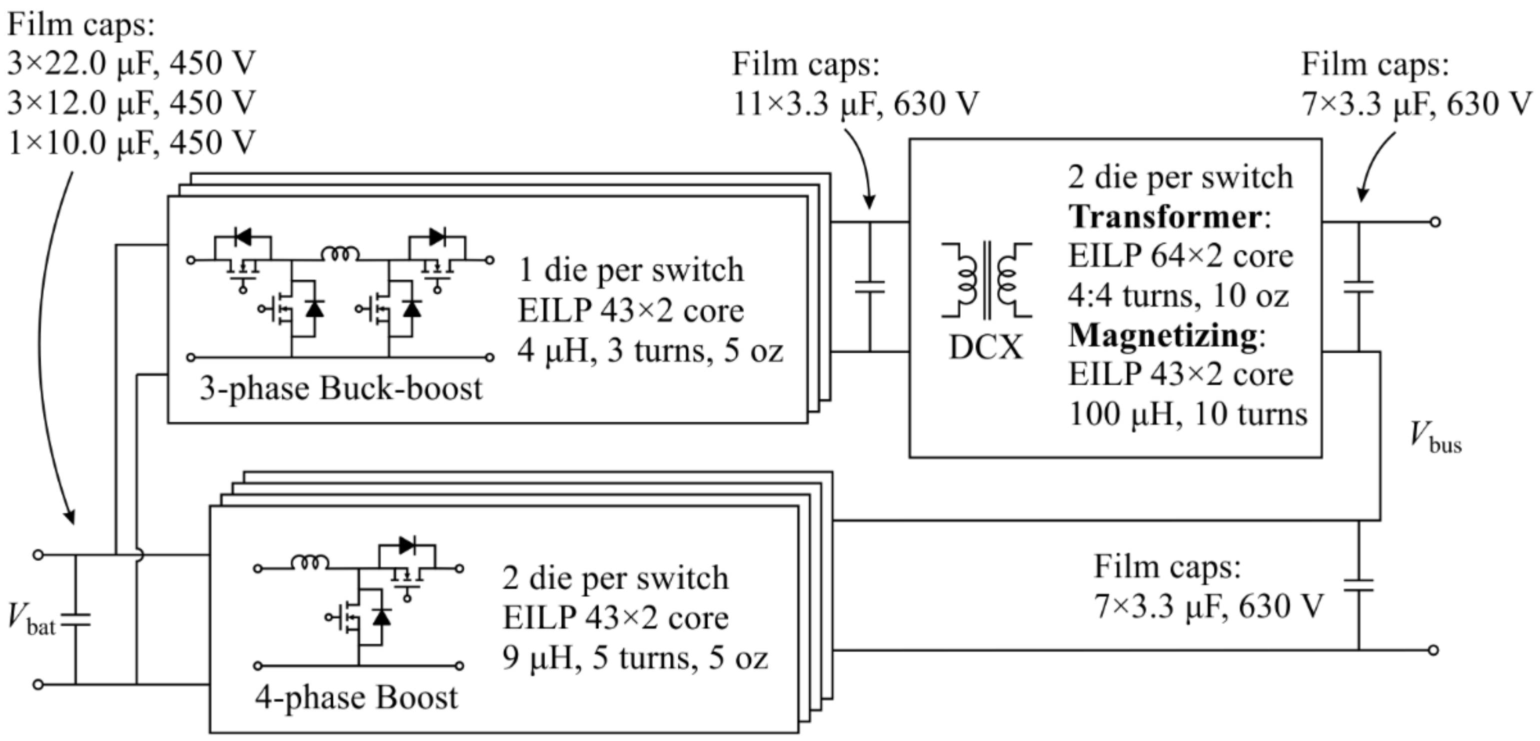

N87 material used for all magnetic cores

All gate drivers are standard low-side drivers with aux supplies and digital isolators

Parameter	Performance
CAFE Q	96.0
Power density	21.3 kW/L
CAFE-weighted MTTF	1,095 khrs
Maximum power	126 kW
Maximum output voltage	1,200 V
Number of SiC-MOSFET die	44
Number of SiC modules	14
System volume	5.9 L
Film capacitor specific density	0.22 J/kW
Ferrite core specific density	2.6 mL/kW
Gravimetric power density	18.7 kW/kg

Module-Level Design: Planar Magnetics

Enhancements in vertical thermal flow

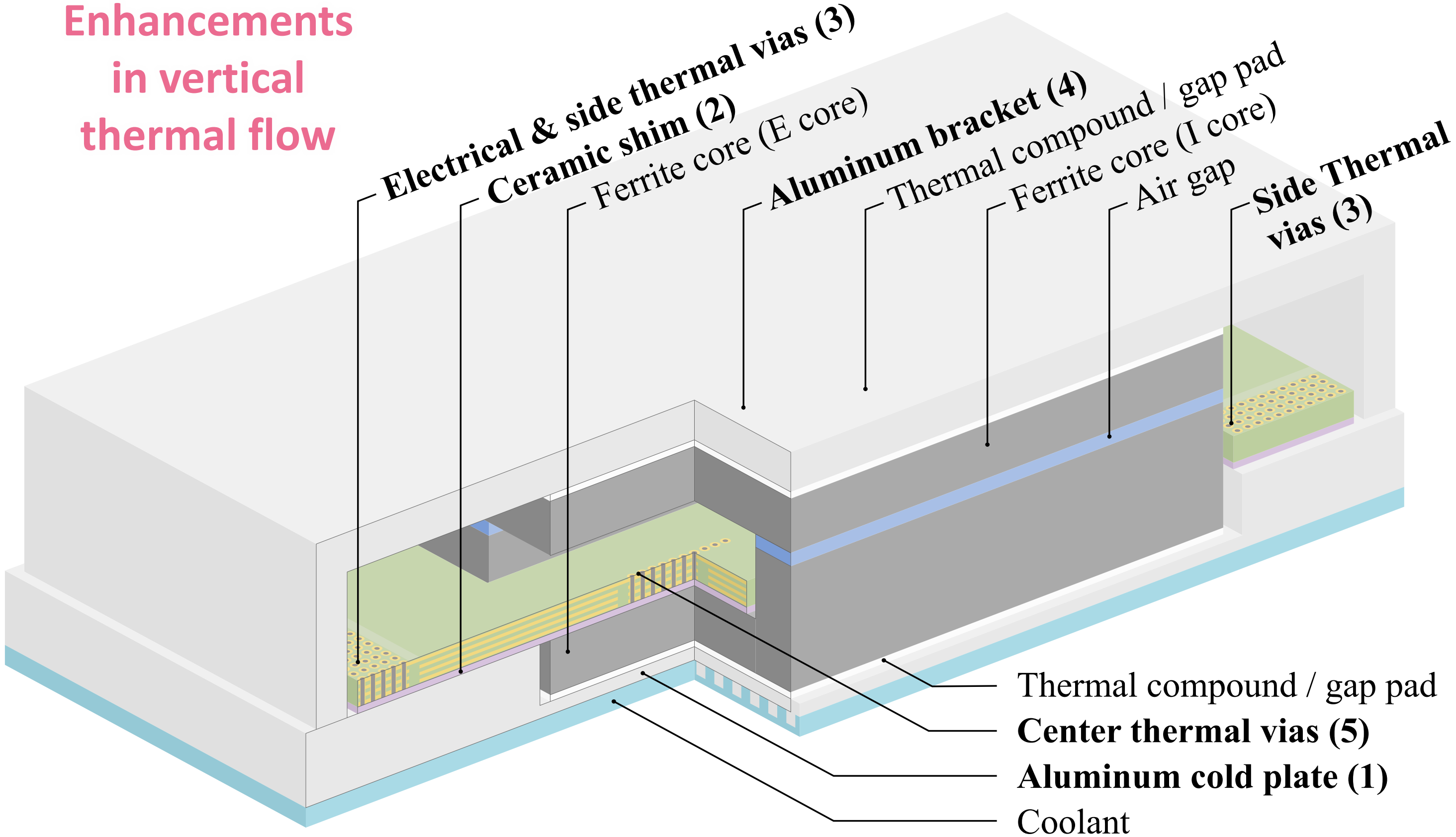

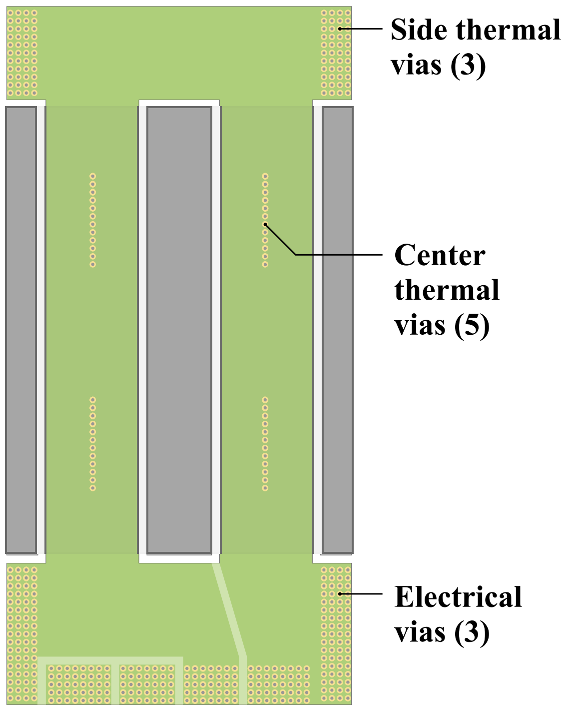

- Thermal management enhancement strategies
- Enable scaling of planar magnetics to 10's of kW

1. Custom aluminum cold plate
2. Thermally-conductive ceramic shim
3. Side thermal vias
4. Aluminum bracket for the I core
5. Center thermal vias

Y. Gao et al., "Modeling and Design of High-Power, High-Current-Ripple Planar Inductors," in IEEE Transactions on Power Electronics, vol. 37, no. 5, pp. 5816-5832, May 2022

Planar Magnetics Optimization and Implementation

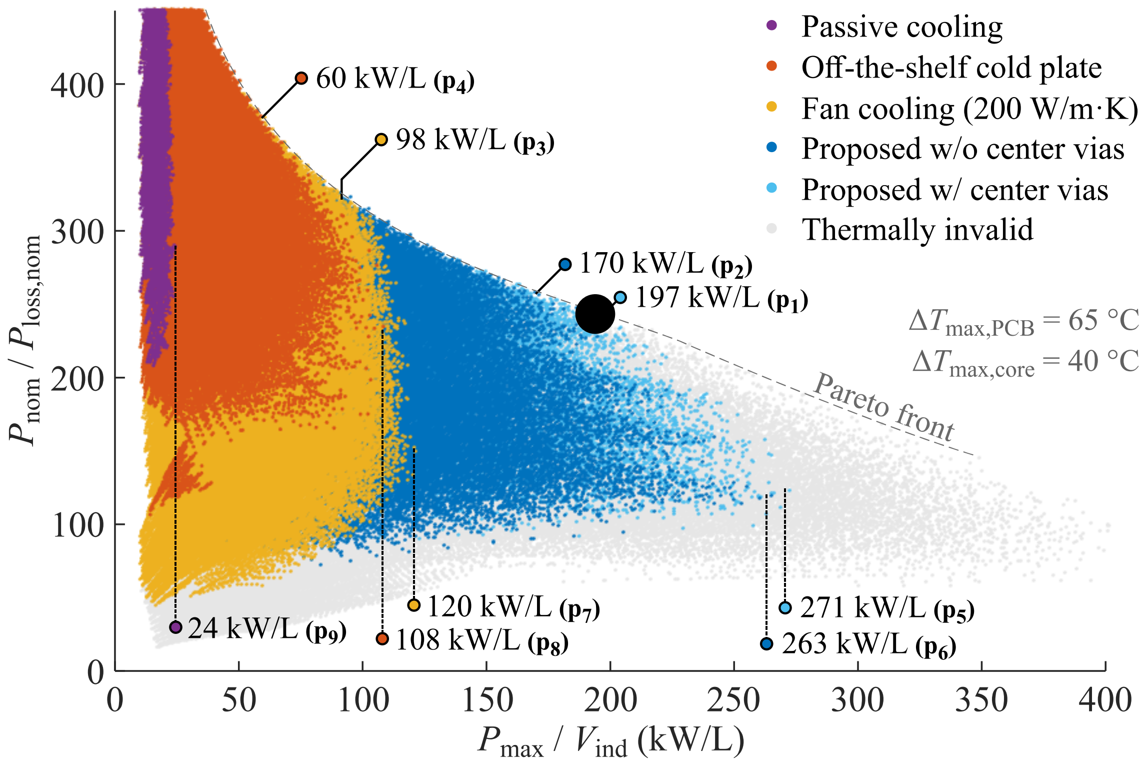

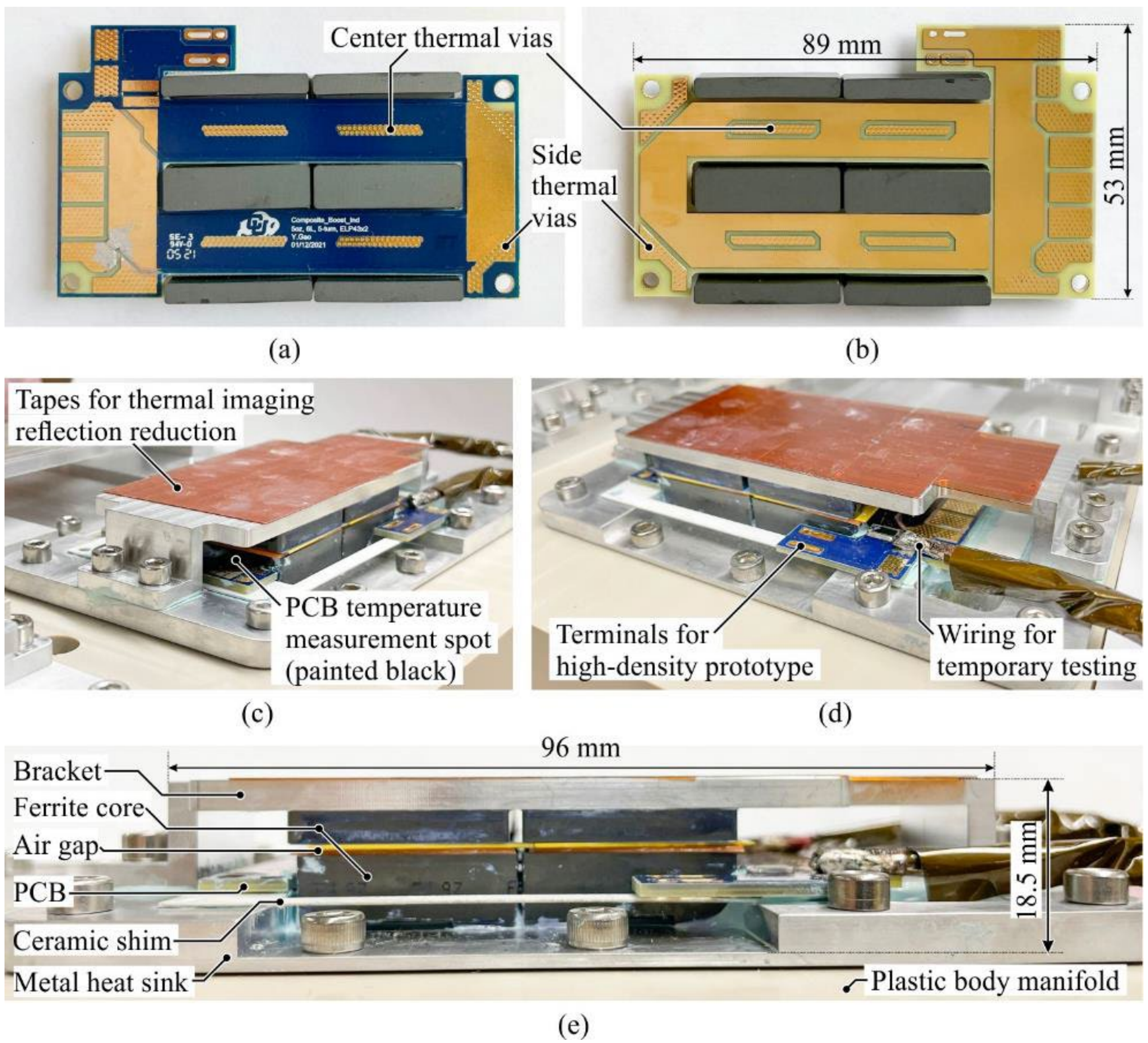

Thermal management enhancements enable substantially higher power density:

- 11× compared to passive cooling
- 2.3× compared to fan cooling
- 2.5× compared to off-the-shelf cold plate

Composite Converter Control Architecture

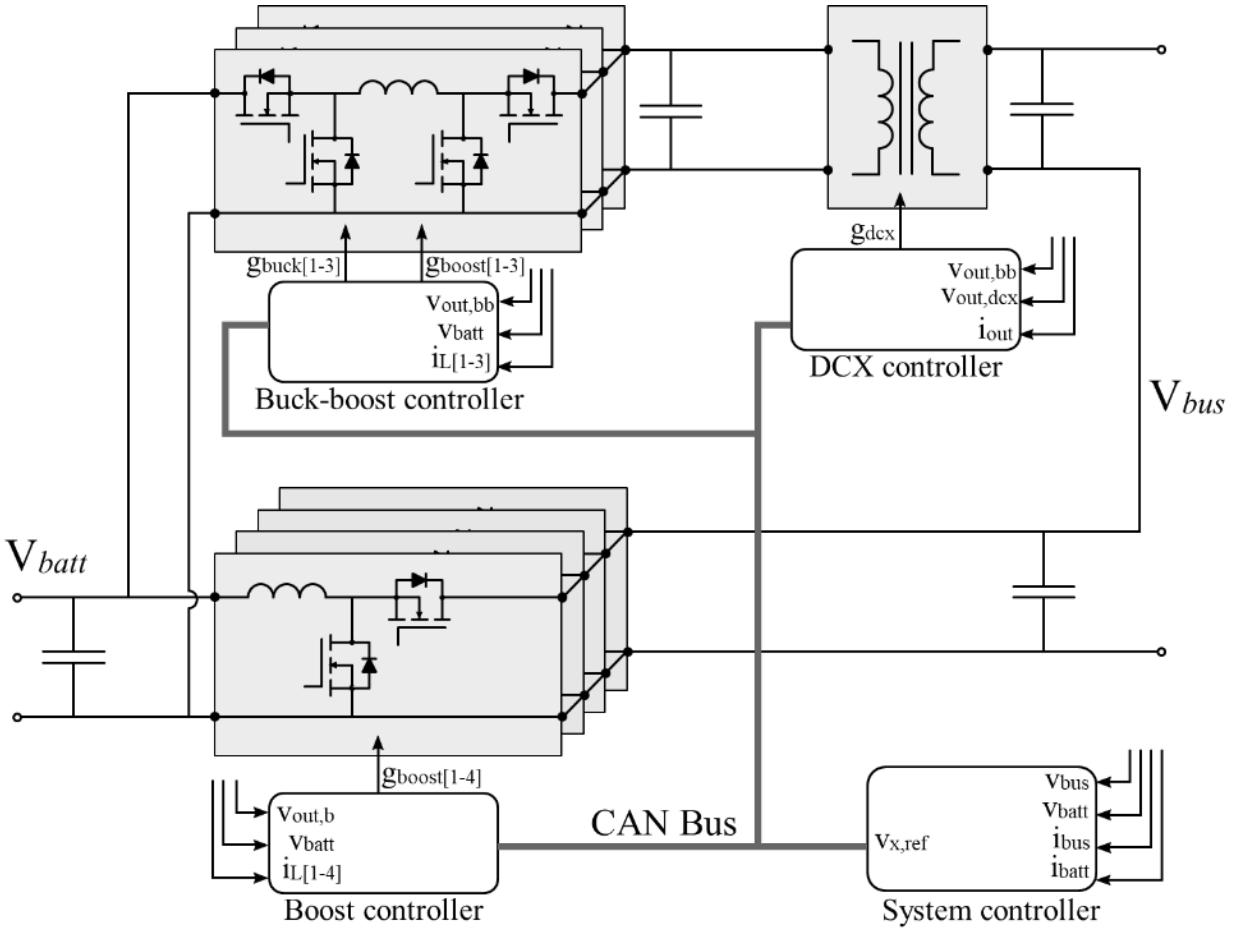

System-level controller

- Bus reference commands
- Mode transitions
- System-level diagnostics, fault handling etc.

Module-level controller

- Current and voltage regulation
- Module-level protections
- Online efficiency optimization

Hierarchical distributed control architecture using TMS320F2837xD dual-core microcontrollers

V. Sankaranarayanan, Y. Gao, R. Erickson and D. Maksimovic, "Online Efficiency Optimization of a Closed-Loop Controlled SiC-Based Bidirectional Boost Converter," *IEEE Trans. on Power El*, 2021.

Module-Level Efficiency-Optimized Control: Minimum-Conduction ZVS-QSW

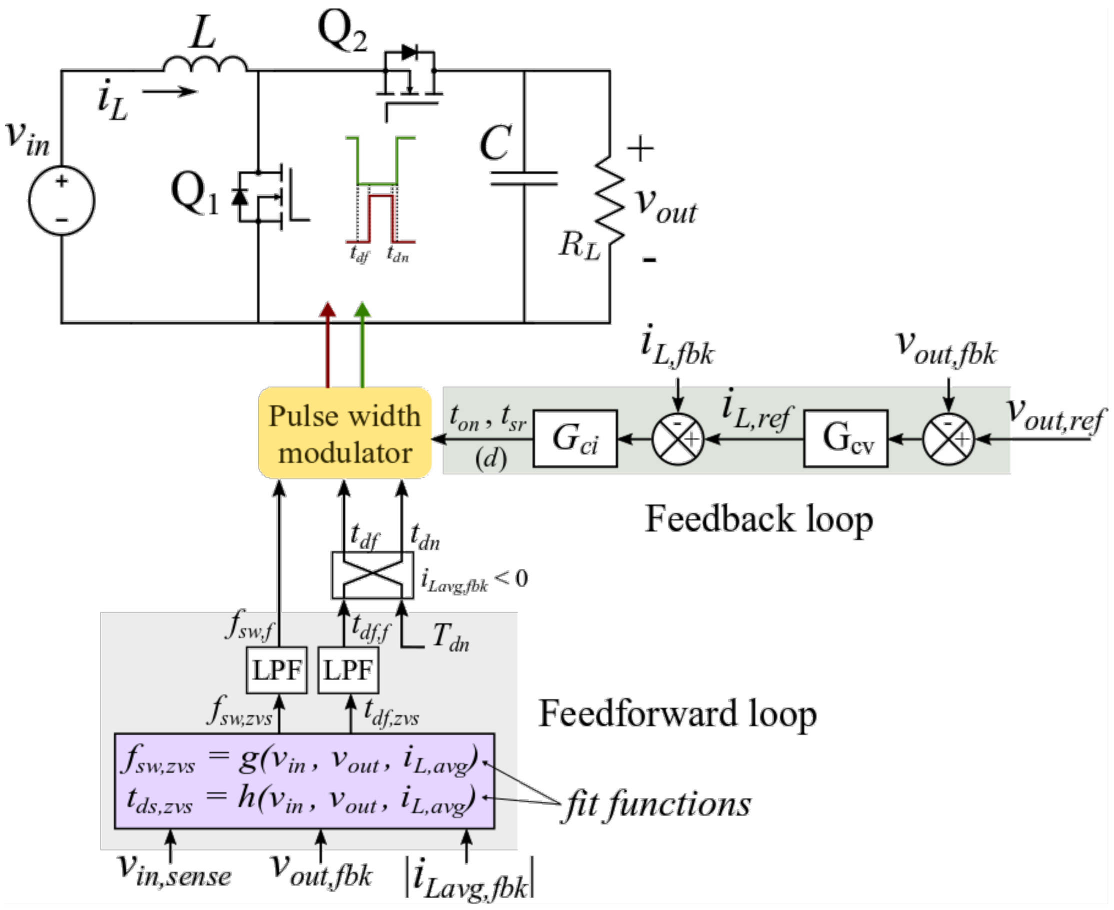

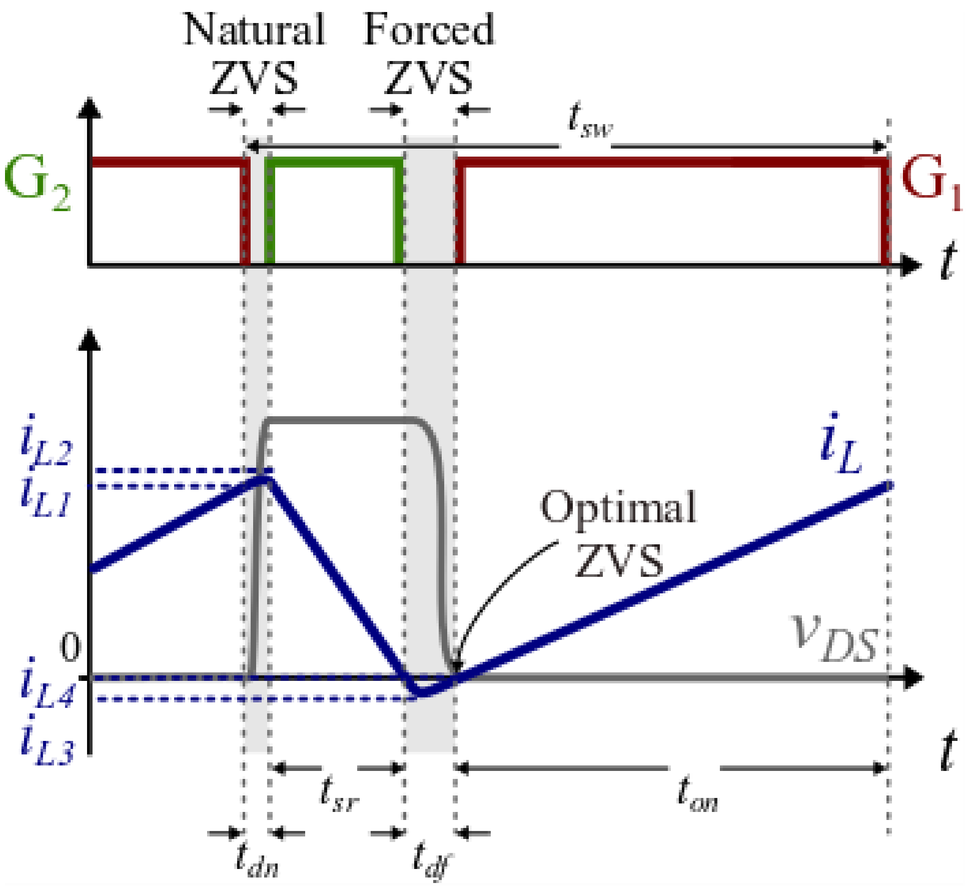

Timing parameters (f_{sw}, t_{df}) adjusted online in response to changes in operating conditions (input voltage, output voltage, and average current)

Minimum-Conduction ZVS-QSW Waveforms

350 → 500 V, m = 1.4, 8.0 kW

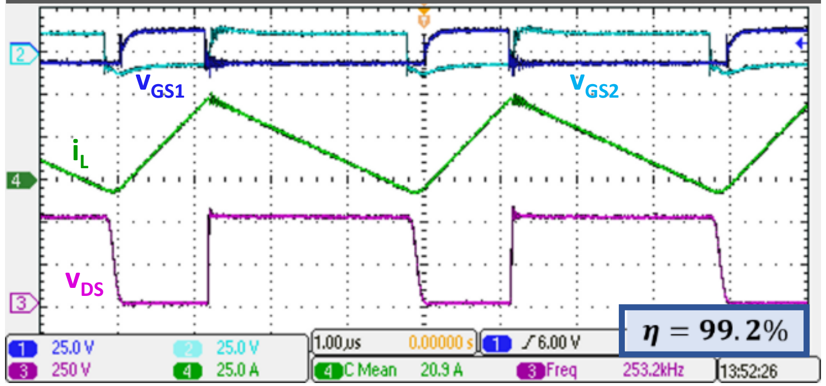

500 → 350 V, m = 0.7, –8.0 kW

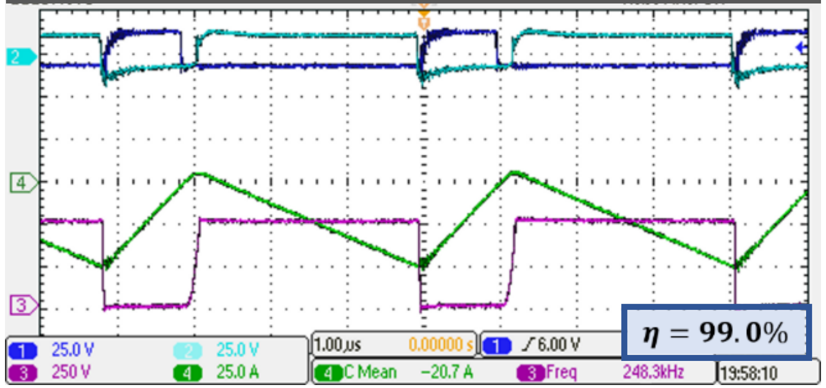

Forward power flow

Waveforms for a half-bridge module with 7.6 µH inductor

Reverse power flow

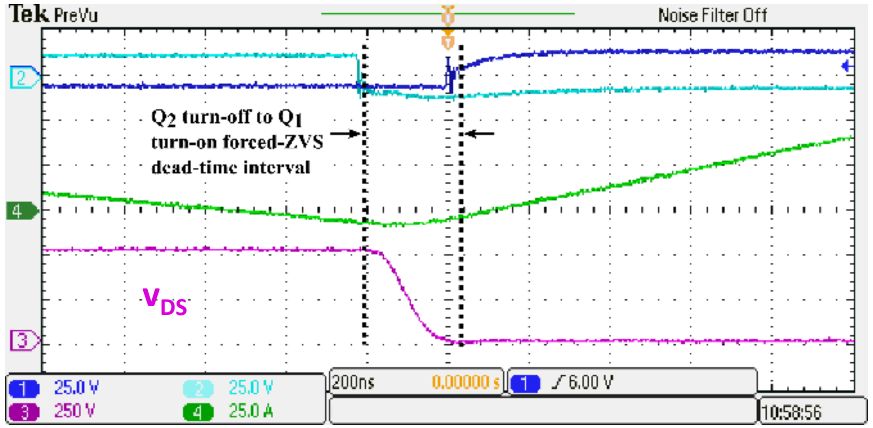

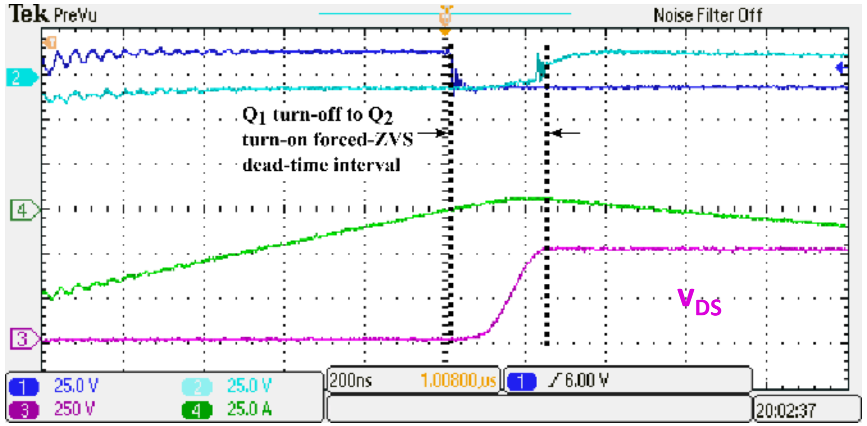

System-Level Control: Operating Modes

Composite converter v_{in},v_{out} plane

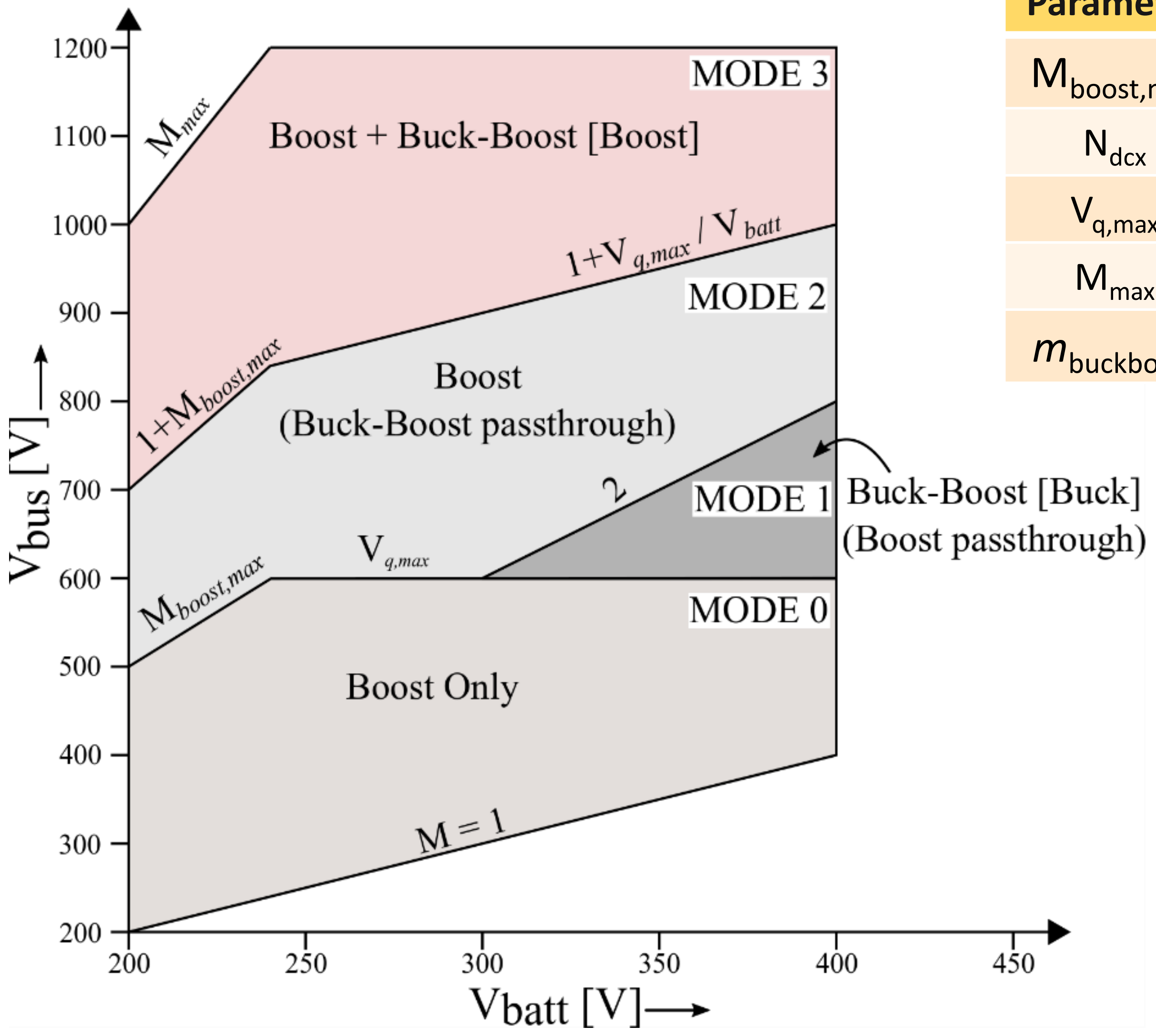

Partial-power module constraints		
Parameter	**Description**	**Value**
$M_{boost,max}$	Maximum conversion ratio for boost	2.5
N_{dcx}	DCX fixed conversion ratio	1
$V_{q,max}$	Maximum output voltage for each module	600V
M_{max}	Maximum system conversion ratio (V_{bus} <= 1200V)	5
$m_{buckboost}$	Conversion ratio range for buck-boost	0.5 - 2.5

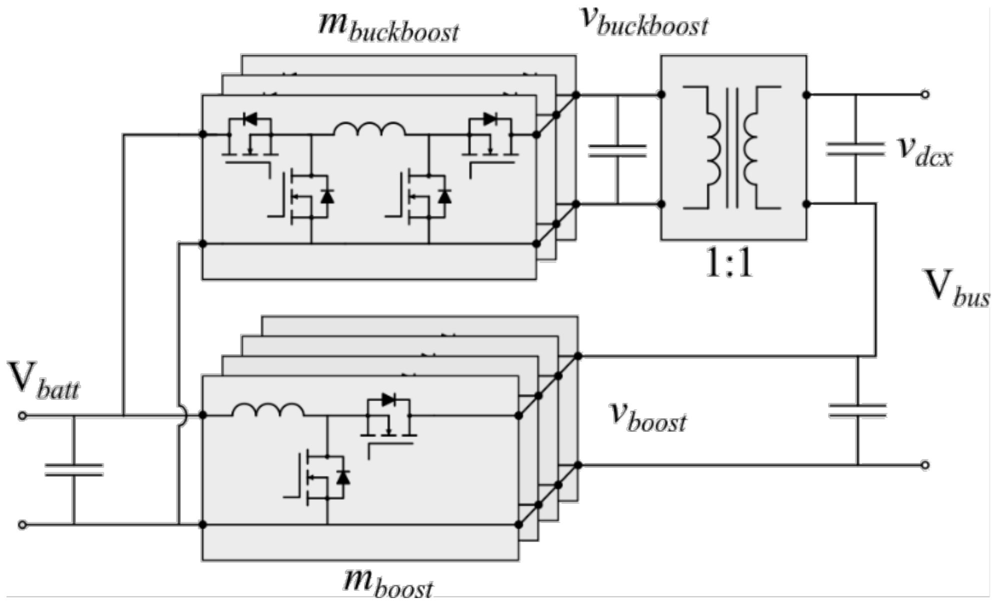

Experimental Results: Mode Transitions

V_{bus} regulated at 700V with v_{BATT} varying from 200V to 400V

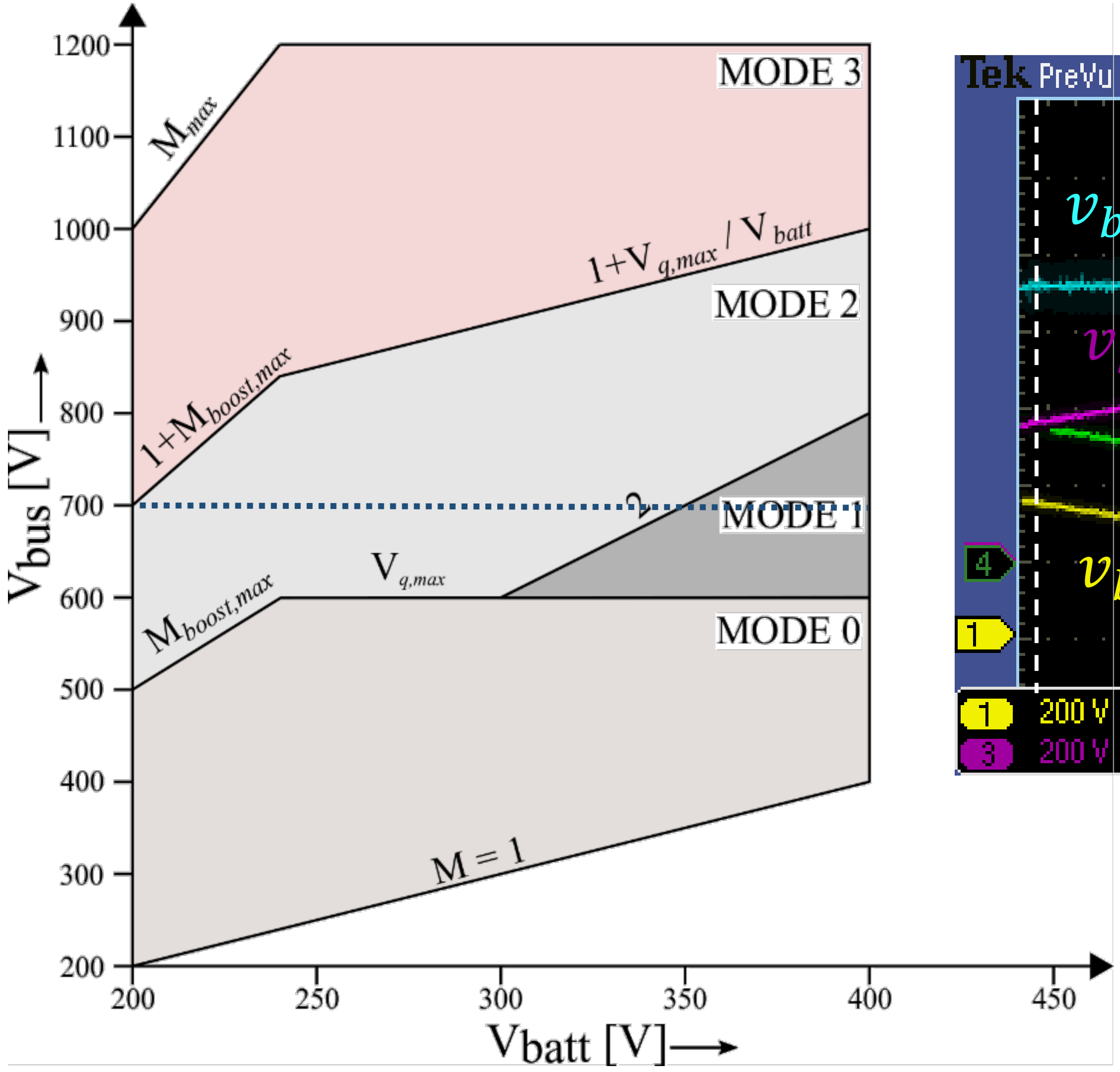

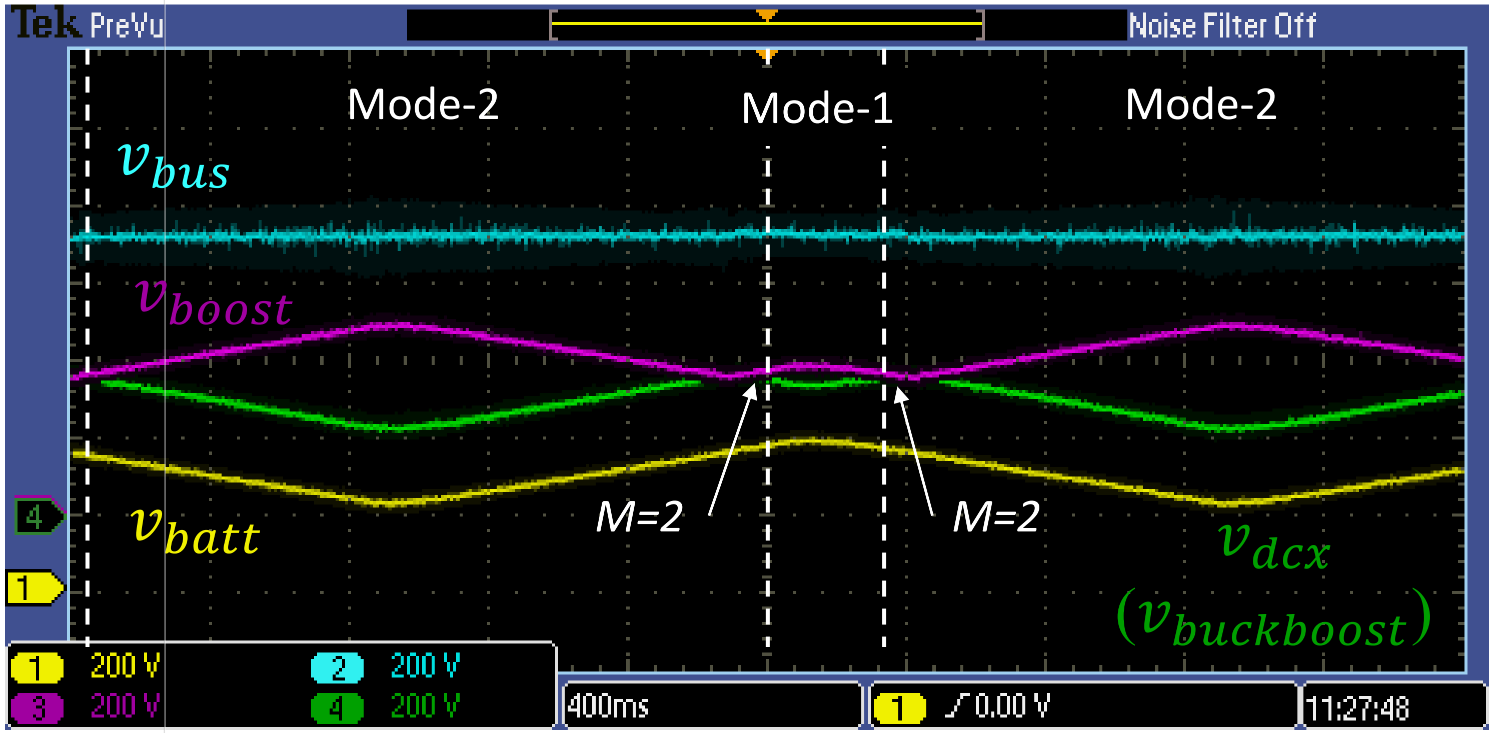

Closed-loop 2-ph operation of boost and buck-boost partial-power modules with module-level efficiency optimization

High-Density System Packaging and Thermal Management

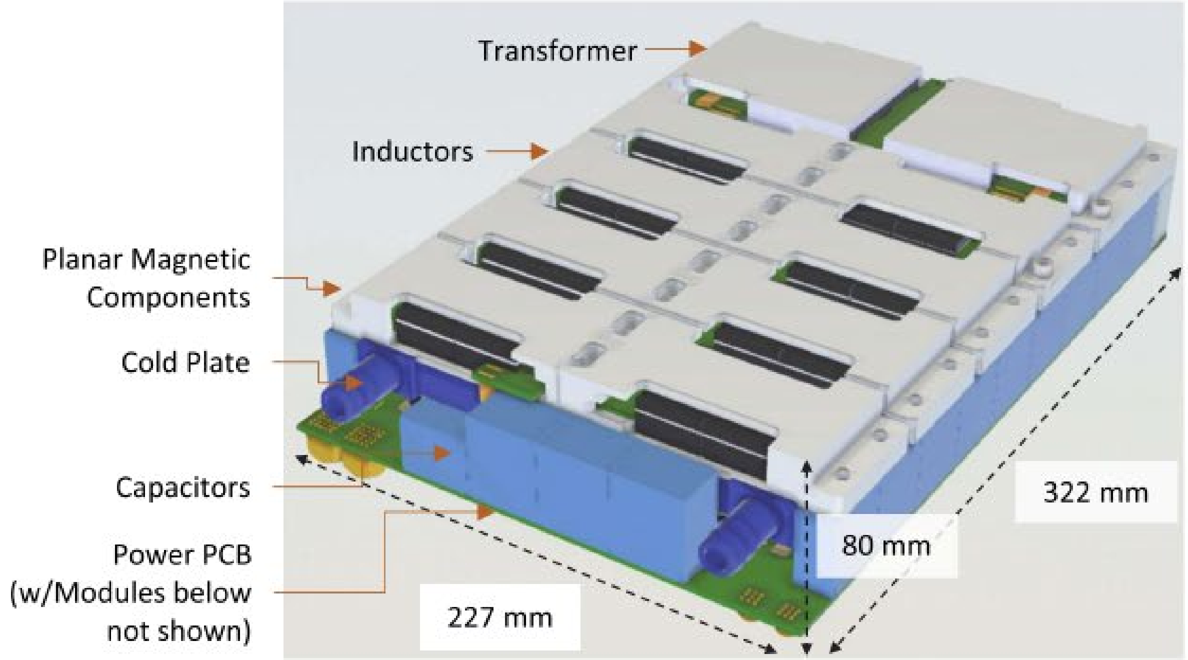

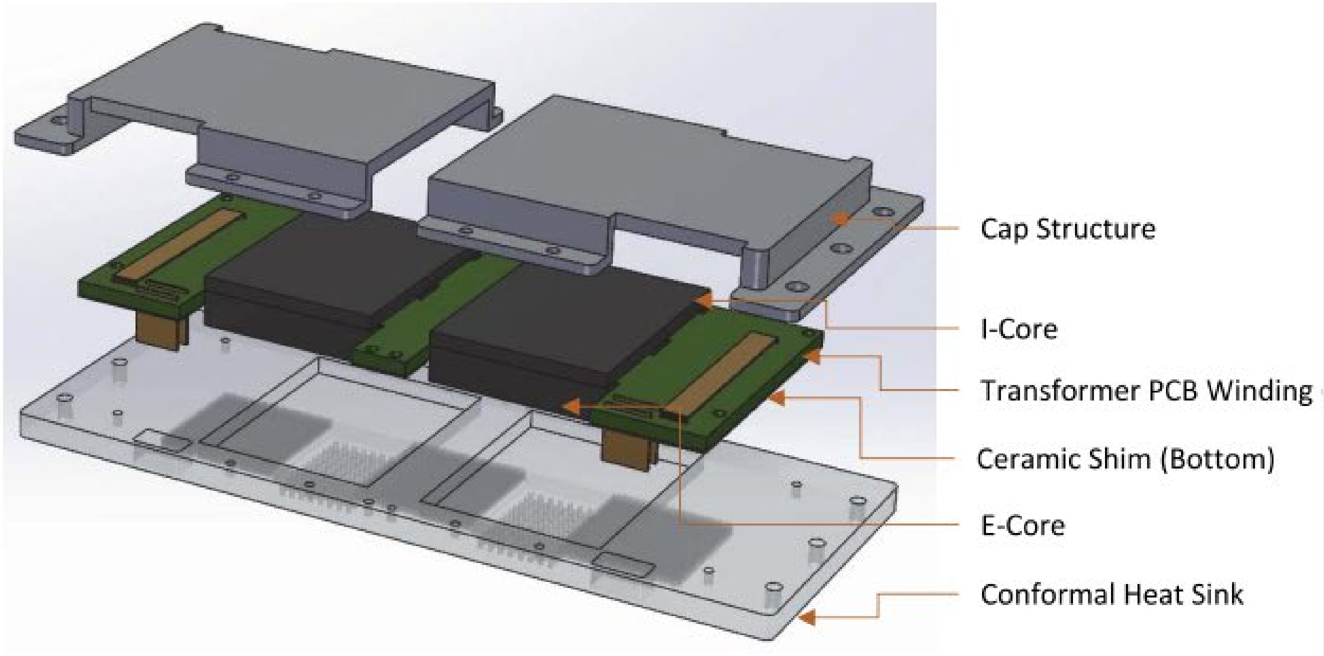

- Double-sided liquid-cooled manifold microchannel (MMC) cold plate
- Planar magnetics on one side, SiC modules on the other

Details of mounting planar magnetics on the cold plate

The system is capable of continuous operation at up to 125 kW with 65^{o} coolant temperature

E. M. Dede et al., "Thermal Design, Optimization, and Packaging of Planar Magnetic Components," in *IEEE Transactions on Components, Packaging and Manufacturing Technology*, vol. 11, no. 9, pp. 1480-1488, Sept. 2021

125 kW, 21.3 KW/L Composite Converter Prototype

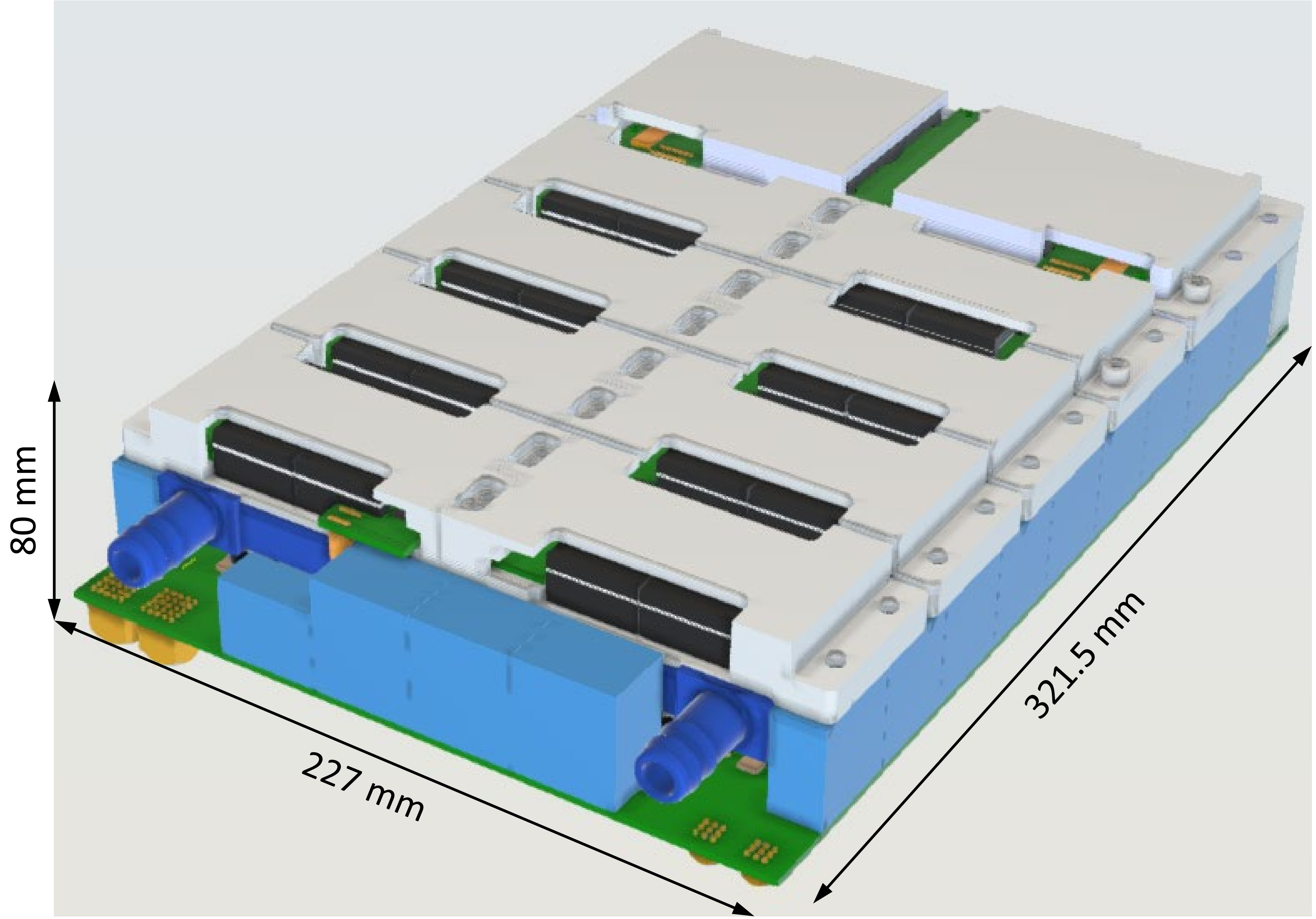

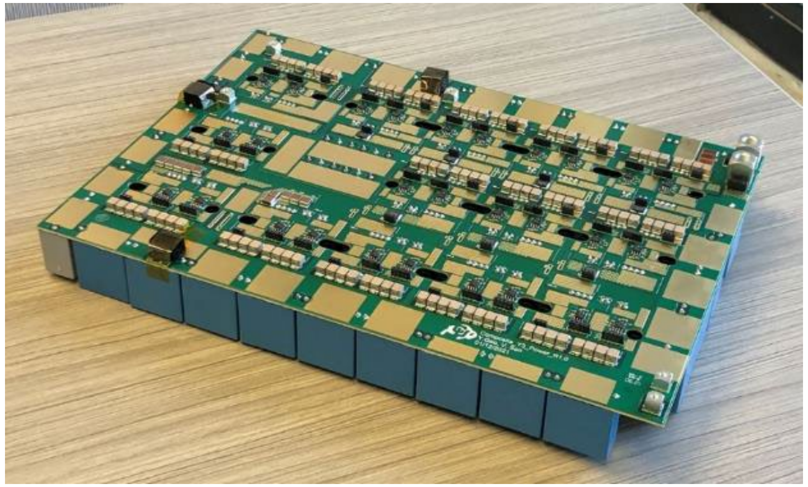

System Experimental Results: Operating Waveforms

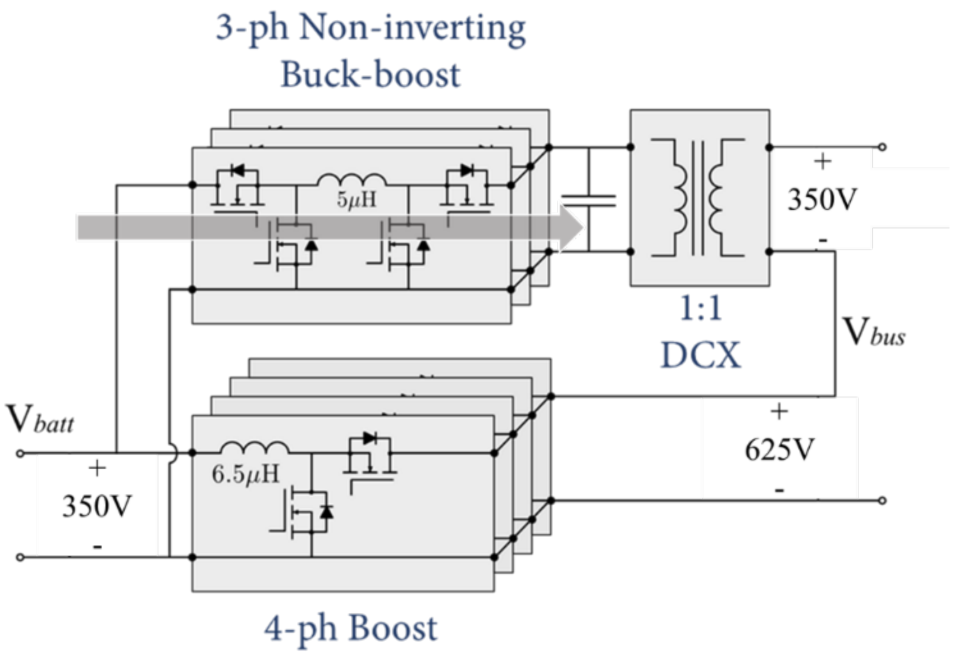

Boost module

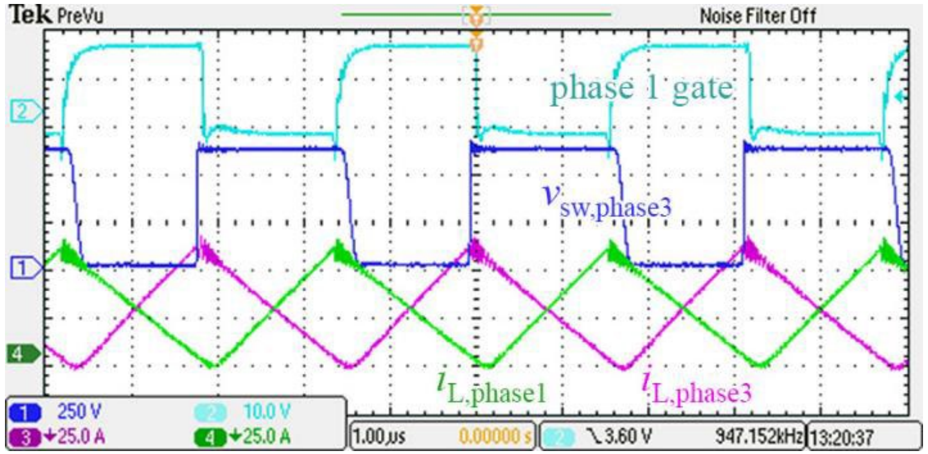

$V_{in} = 350$ V, $V_{out} = 975$ V, $P_{out} = 26$ kW, $\eta = 98.7\%$, $Q = 76$

DCX DAB module

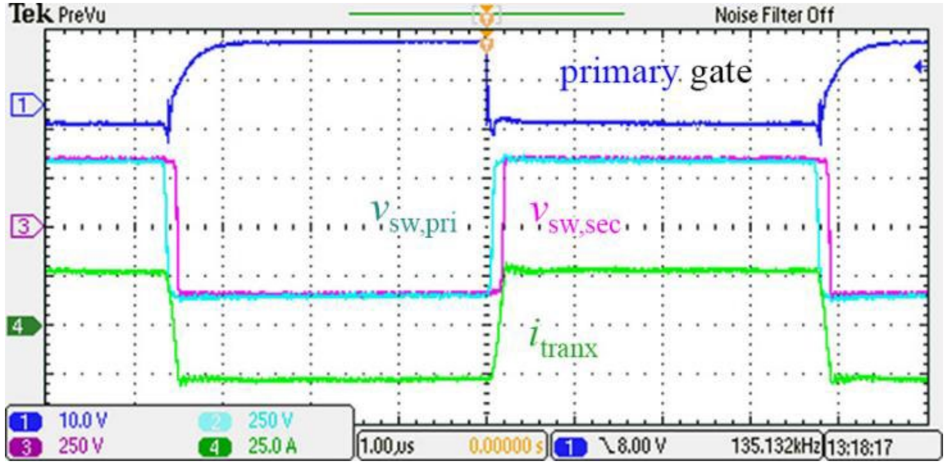

$V_{in} = 350$ V, $V_{out} = 975$ V, $P_{out} = 51$ kW, $\eta = 98.4\%$, $Q = 62$

DCX DAB module

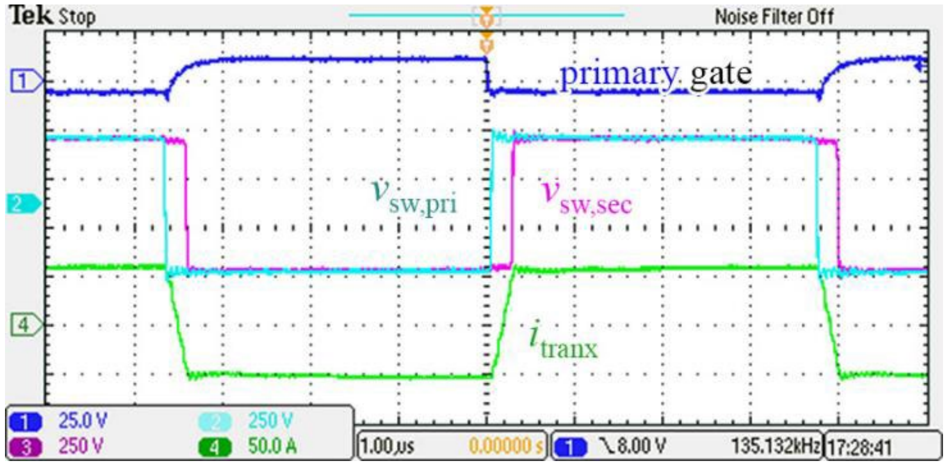

Experimental Results: Boost Module CAFE-weighted *Q*

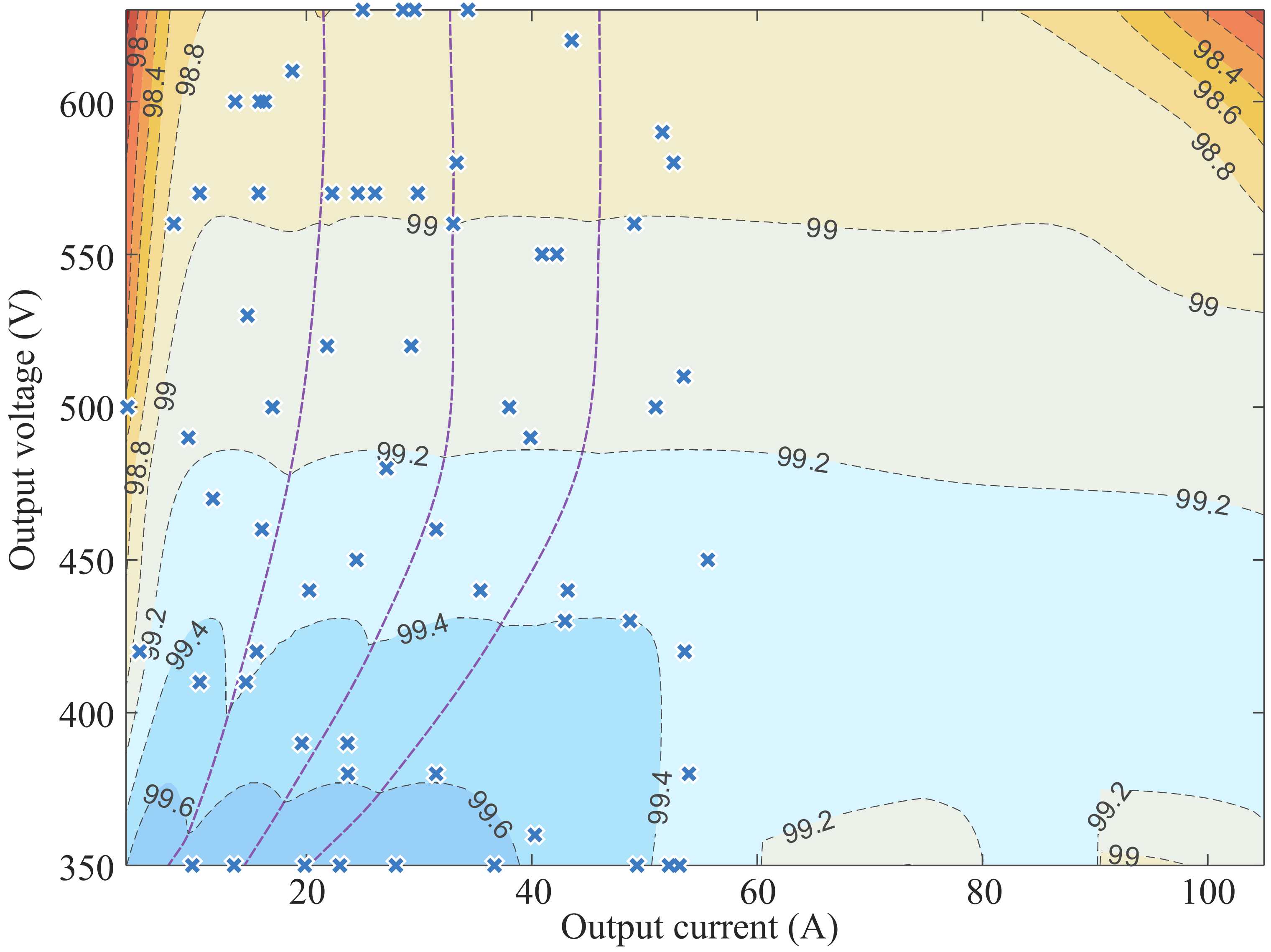

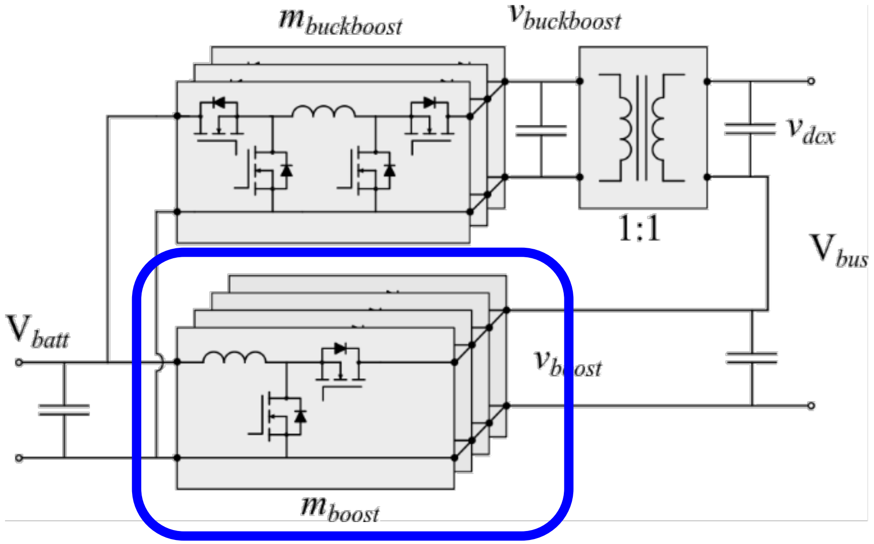

- **55 step-up points**
  9 pass-through points
- Efficiency-optimized control, including phase-shedding
- Averaged power: 12.8 kW
- Averaged loss: 95.8 W
- **CAFE Q: 133.1**

Experimental Results: Buck-Boost Module CAFE-weighted Q

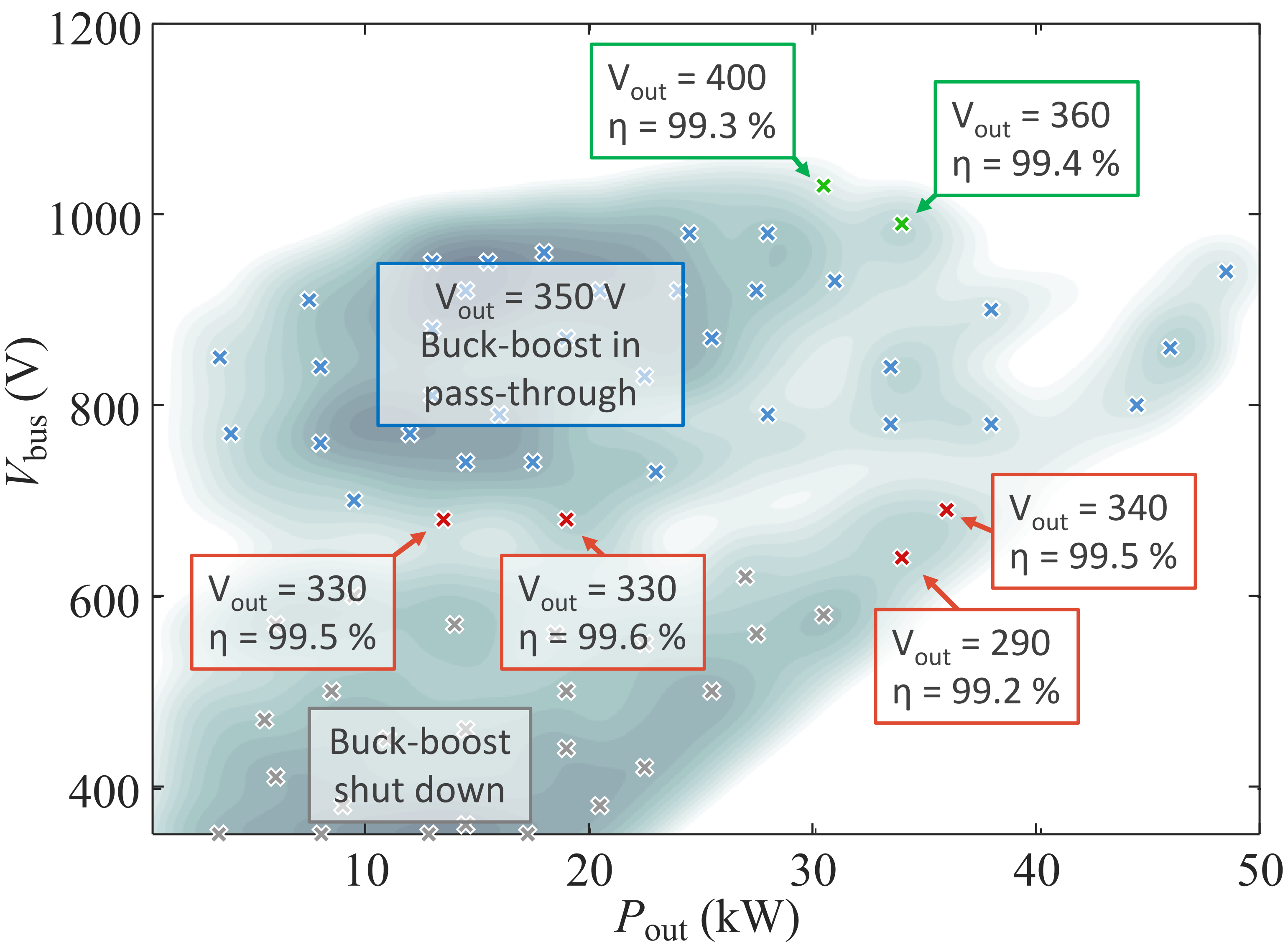

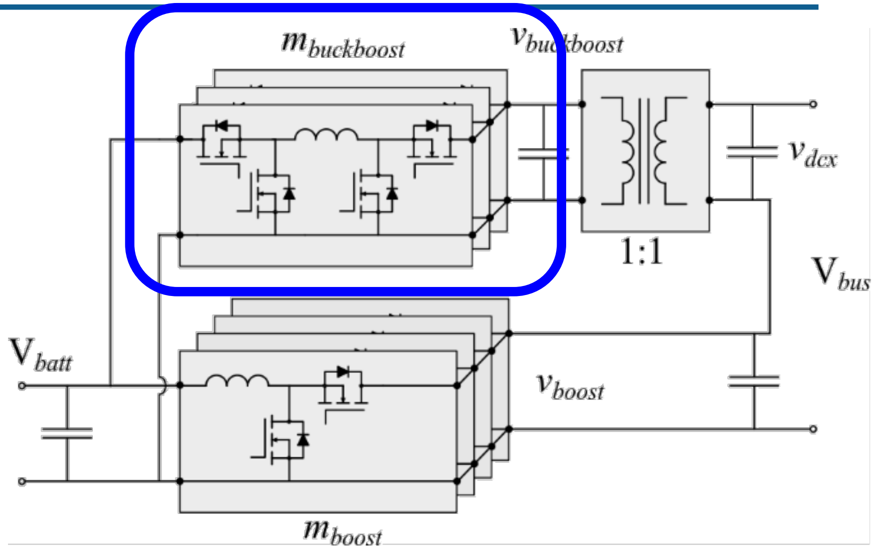

- **6 step-up/down points**
  34 pass-through points
  24 shut-down points
- Efficiency-optimized control, including phase-shedding
- Averaged power: 4.4 kW
- Averaged loss: 6.9 W
- **CAFE Q: 642.4**
  (168.9 for step-up/down points)

Experimental Results: DAB DCX Module CAFE-weighted Q

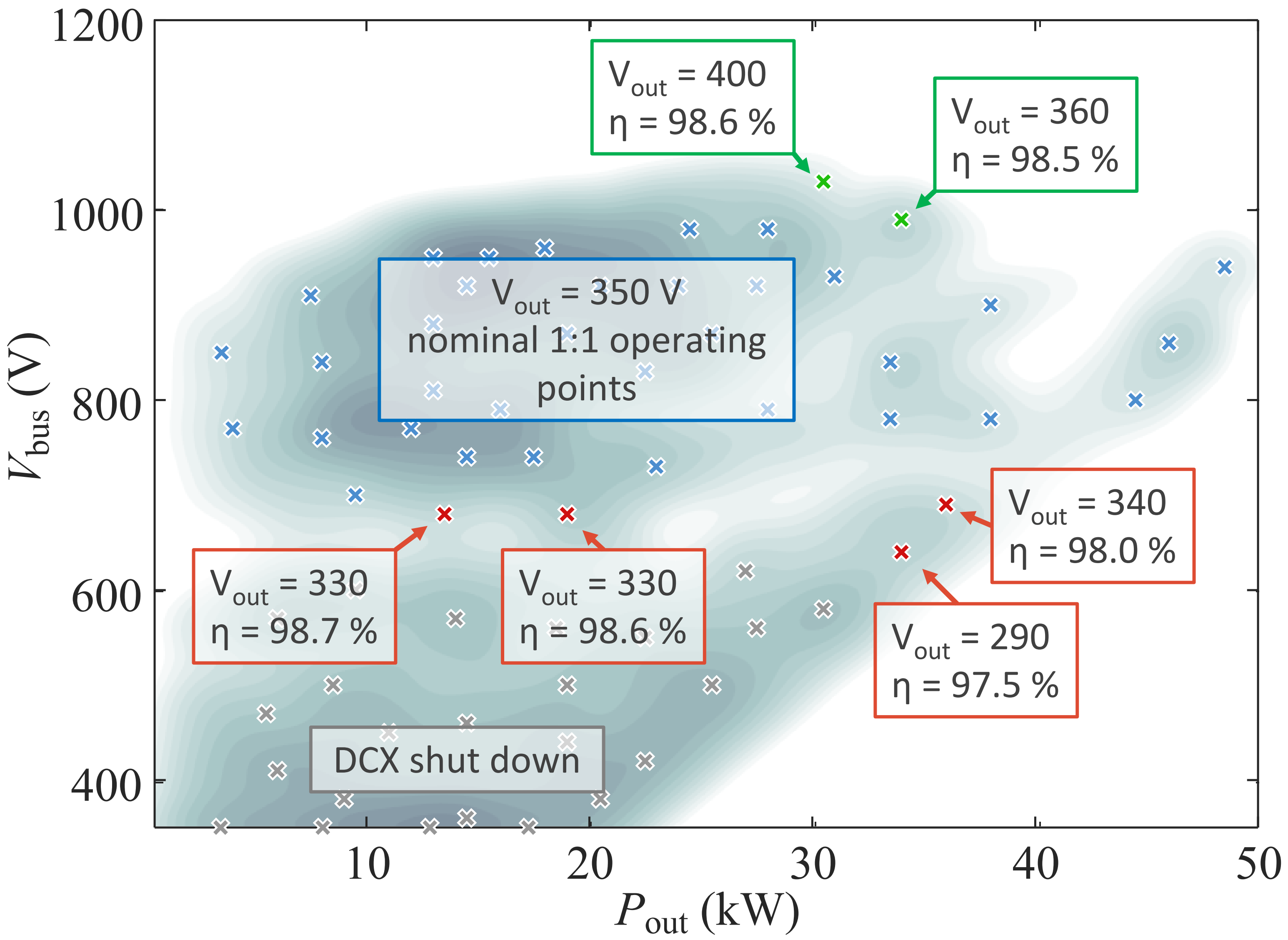

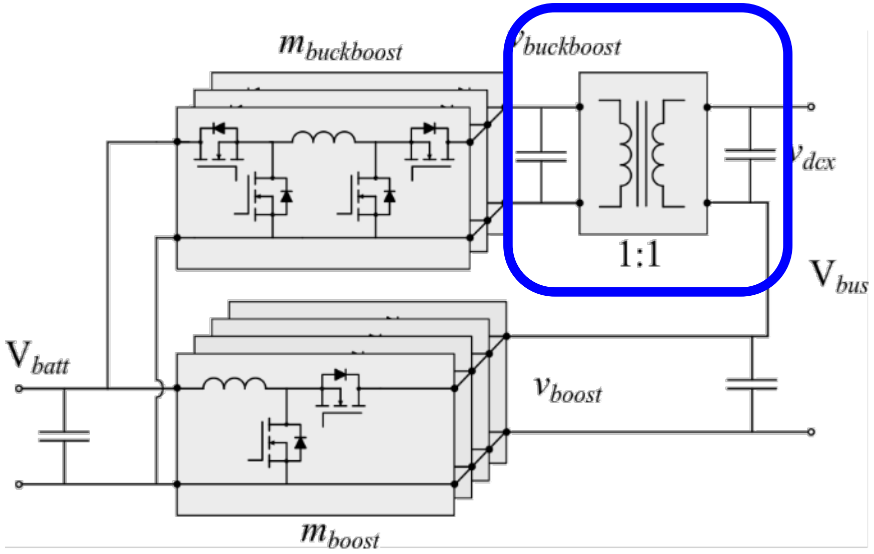

- **34 nominal 1:1 (350 V) points**
  6 non-350 V points
  24 shut-down points
- Averaged power: 4.4 kW
- Averaged loss: 71.5 W
- **CAFE Q: 62.1**

Drive-cycle CAFE-weighted System Q and Efficiency

	Averaged power	Averaged loss	CAFE Q
Boost	12.75 kW	95.8 W	133.1
Buck-boost	4.43 kW	6.9 W	642.4
DCX	4.43 kW	71.5 W	62.1
System	**17.19 kW**	**174.2 W**	**98.6**

$$\eta = 99\%$$

*Corporate average fuel economy (CAFE): a weighted drive cycle defines a typical system operating pattern

Comparison of SiC based Converters for Electric Drivetrain Applications

	SiC conventional boost	SiC composite boost	Improvements over conventional
Max output voltage	1200 V	1200 V	
Switching frequency	60 kHz	**100 – 350 kHz**	**2-5x higher**
Magnetics	Wire-wound	**Planar**	**2x smaller**
Capacitors	Film	Film	**4x smaller**
Power devices	1700 V SiC	**900 V SiC**	
SiC semi area	1,600 mm^2	1,400 mm^2	≈ same
CAFE Q	63.5	**98.6**	**1.5x higher**
CAFE Efficiency	98.4%	**99.0%**	
Power density	9.9 kW/L	**21.3 kW/L**	**2.2x higher**
Calculated MTTF	304 khrs	**1,095 khrs**	**3.6x higher**

MTTF Calculations

SiC MOSFET

Time-dependent dielectric breakdown (TDDB)

$$MTTF_{TDDB} = \exp\left[\frac{E_a}{k}\left(\frac{1}{T} - \frac{1}{T_{base,sw}}\right)\right] MTTF_{base}$$

Temperature cycling effect (failure of bonding wires)

- Requires time-domain information
- Only considered in the final optimization stage

Number of cycles to fail: $N_f = A \cdot \Delta T_j^{-\alpha} \cdot \exp\left[\frac{E_a}{k \cdot T_{j,avg}}\right]$

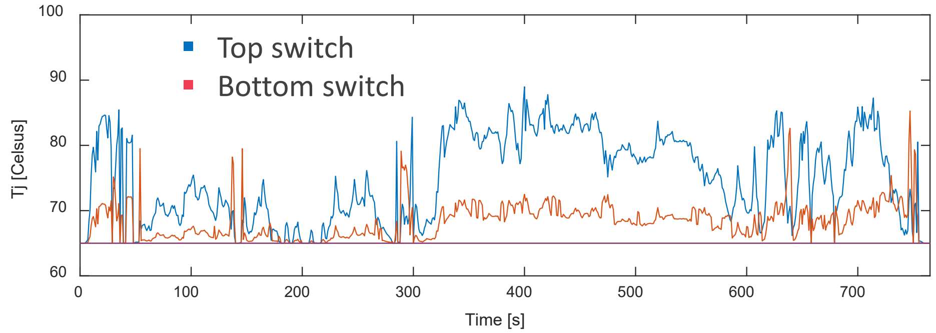

◀ Example: simulated boost converter switch T_j in the highway drive cycle

Gate driver IC

- Based on manufacturer published data
- Temperature dependent to switching frequency & number of die

$$MTTF_{ic} = \exp\left[\frac{E_a}{k}\left(\frac{1}{T} - \frac{1}{T_{base,ic}}\right)\right] MTTF_{ic,40℃}$$

Capacitors

- Based on manufacturer published data
- With consideration of the voltage utilization rate and temperature rise

$$MTTF_{cap} = \left[\sum_i \frac{\pi_{v,i}\pi_{t,i}}{MTTF_{cap,unit}}\right]^{-1}$$

Conclusions: High-Density, High-Efficiency Power Electronics

- Architectures that make best use of wide-bandgap device capabilities
- Design optimization and control techniques
- Packaging and system integration techniques
- Power and voltage scaling of composite architectures and planar magnetics
- “Simple” may not always be the best approach in power electronics

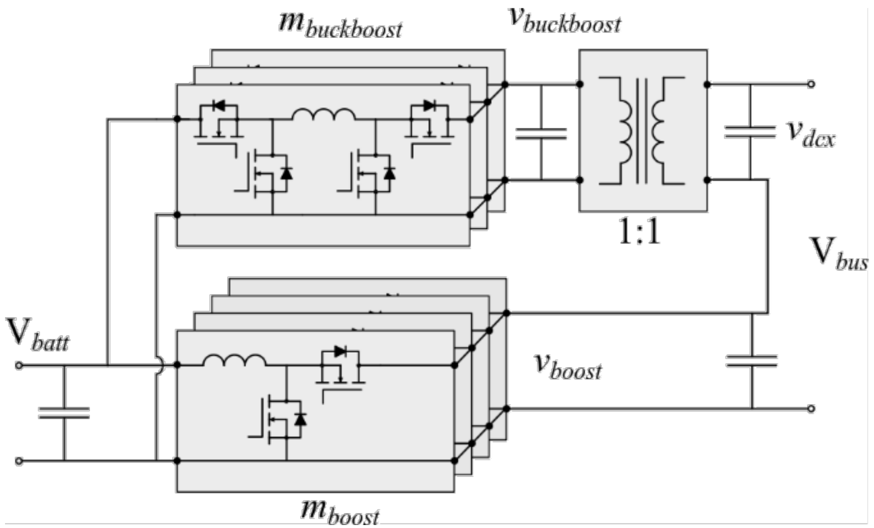

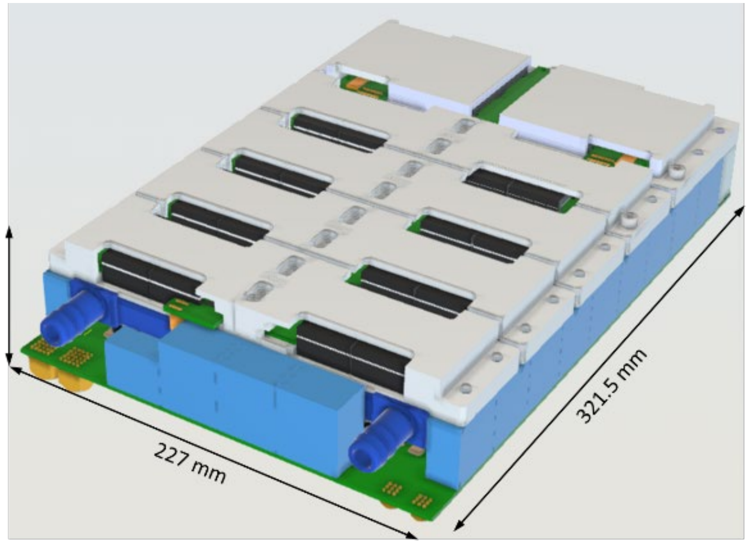

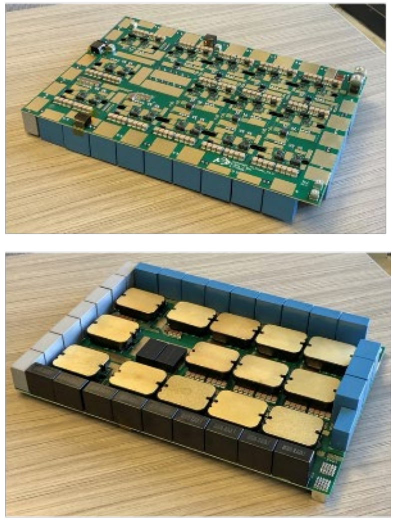

Acknowledgments

Bob Erickson (PI), Yucheng Gao, Vivek Sankaranarayanan

Ercan Dede, Yuqing Zhou, Feng Zhou

Mariko Shirazi

Barry Mather

Sayan Seal, Brandon Passmore, Kraig Olejniczak

ARPA-E CIRCUITS program directed by Dr. Isik Kizilyalli

References

- Y. Gao et al., "Modeling and Design of High-Power, High-Current-Ripple Planar Inductors," in IEEE Transactions on Power Electronics, vol. 37, no. 5, pp. 5816-5832, May 2022.
- V. Sankaranarayanan, Y. Gao, R. W. Erickson and D. Maksimovic, "Online Efficiency Optimization of a Closed-Loop Controlled SiC-Based Bidirectional Boost Converter," in IEEE Transactions on Power Electronics, vol. 37, no. 4, pp. 4008-4021, April 2022.
- E. M. Dede et al., "Thermal Design, Optimization, and Packaging of Planar Magnetic Components," in IEEE Transactions on Components, Packaging and Manufacturing Technology, vol. 11, no. 9, pp. 1480-1488, Sept. 2021.
- Y. Gao, V. Sankaranarayanan, R. W. Erickson and D. Maksimovic, "Soft Startup Strategies for DAB-Based DCX in Composite Converters," 2020 IEEE Energy Conversion Congress and Exposition (ECCE), 2020, pp. 6130-6135.
- Y. Gao, V. Sankaranarayanan, R. W. Erickson and D. Maksimovic, "Analysis and Attenuation of Differential-Mode Resonances due to Winding Capacitances in High-Power Planar Transformers," 2020 IEEE Applied Power Electronics Conference and Exposition (APEC).
- V. Sankaranarayanan, Y. Gao, R. W. Erickson and D. Maksimovic, "Online Efficiency Optimization of a Closed-Loop Controlled SiC-Based Boost Converter," 2020 IEEE Applied Power Electronics Conference and Exposition (APEC), pp. 285-291.
- V. Sankaranarayanan, M. Shirazi, Y. Gao, A. Ghosh, R. W. Erickson and D. Maksimovic, "Controller Hardware-in-the-Loop Validation of a Modular Control Architecture for a Composite DC-DC Converter," 2019 20th Workshop on Control and Modeling for Power Electronics (COMPEL).
- Y. Gao, V. Sankaranarayanan, E. M. Dede, A. Ghosh, D. Maksimovic and R. W. Erickson, "Drive-Cycle Optimized 99% Efficient SiC Boost Converter Using Planar Inductor with Enhanced Thermal Management," 2019 20th Workshop on Control and Modeling for Power Electronics (COMPEL).
- H. Kim et al., "SiC-MOSFET composite boost converter with 22 kW/L power density for electric vehicle application," 2017 IEEE Applied Power Electronics Conference and Exposition (APEC), 2017.
- H. Chen, H. Kim, R. Erickson and D. Maksimović, "Electrified Automotive Powertrain Architecture Using Composite DC–DC Converters," in IEEE Transactions on Power Electronics, vol. 32, no. 1, pp. 98-116, Jan. 2017.
- H. Chen, K. Sabi, H. Kim, T. Harada, R. Erickson and D. Maksimovic, "A 98.7% Efficient Composite Converter Architecture With Application-Tailored Efficiency Characteristic," in IEEE Transactions on Power Electronics, vol. 31, no. 1, pp. 101-110, Jan. 2016.

Thank you!